Department of Pharmacy, Faculty of Health Sciences
University of Tromsø The Arctic University of Norway

Characterization of the cell secretomes from undifferentiated and chondro-induced stem cells

—

Jerusalem Yonas Hambissa
Supervisor: Professor Inigo Zubiavrre Martinez
Thesis for the degree Master of Pharmacy, May 2015

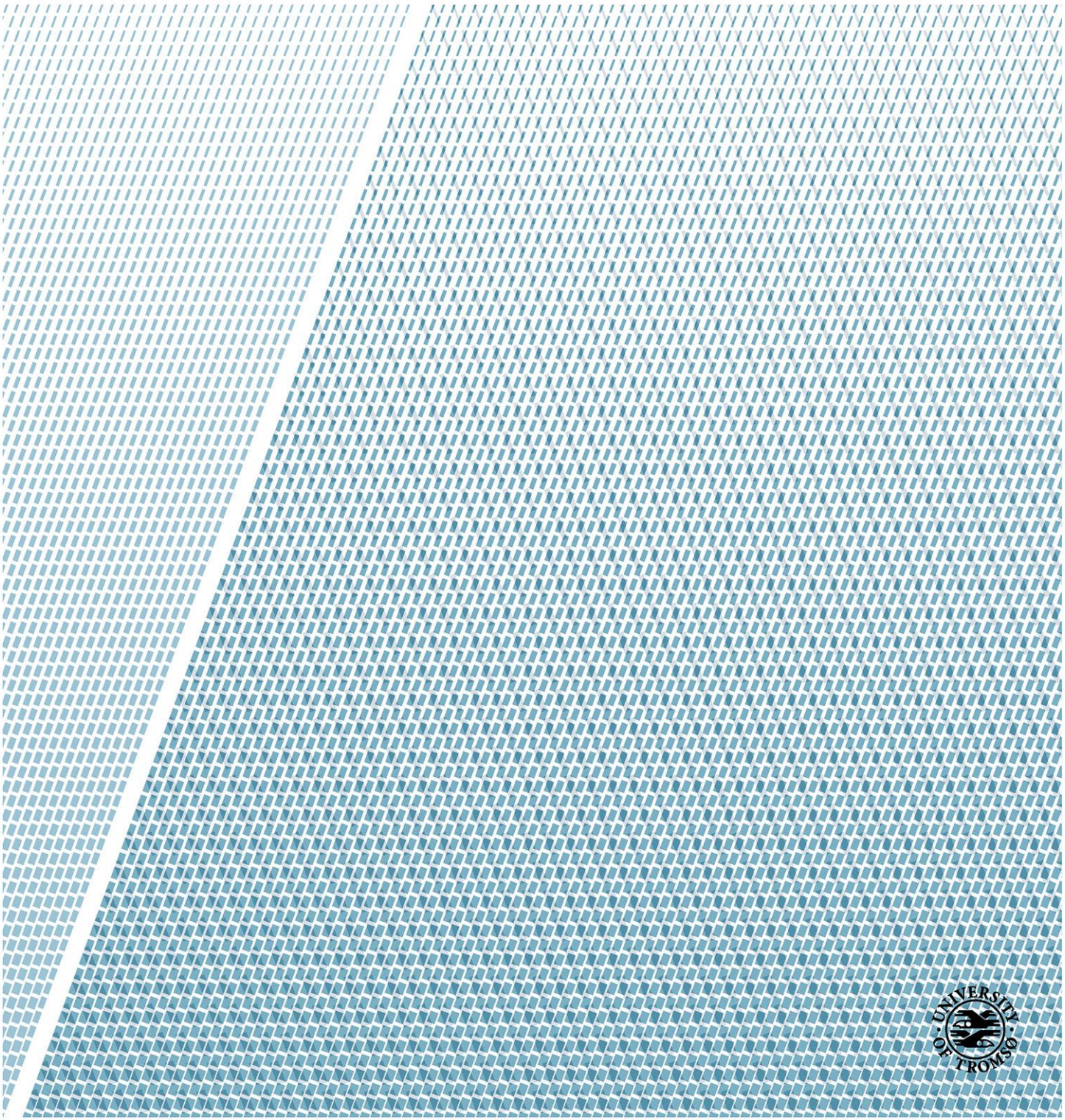

Abstract

Background: Articular cartilage is an essential part of the skeletal system. It provides a frictionless surface for smooth pain-free articulation and limits the load applied to subchondral bone during joint movement. Articular cartilage is an avascular and aneural tissue without lymphatic vessels. Due to this unique nature, articular cartilage has poor self-repair capacity. Therefore, minor cartilage defect often leads to Osteoarthritis (OA). OA is considered one of the most common forms of arthritis and a major cause of physical disability amongst non-hospitalized adults, particularly in the aging population. Various treatment methods have been developed, but all bear limitations. Cellular therapy, where mesenchymal stem cells are used to reconstruct articular cartilage has shown encouraging results.

Aim: In this study, we have compared the chondrogenic potential of mesenchymal-like stem cells (MSCs) from Hoffa fat pad (HFP) and umbilical cords (UC). Scaffold-free 3D cultures were used to induce chondrogenic differentiation and final tissue products were checked by histological and biochemical assays. Proteomic analyze of HFPSC secretome was used to check changes in inflammatory and immune-modulatory responses before and after differentiation.

Results: Isolated cells were plastic-adherent, highly proliferative and expressed surface markers according to MSCs phenotype. The mean GAG/DNA ratio was very similar for both HFPSCs and MCSCs. Cartilage spheroids of HFPSCs showed more intense alcian blue staining than MCSCs and had better cartilage-like morphology. Proteomics analyze of the supernatant of HFPSCs showed no differences in expression of inflammatory immune-modulatory molecules between monolayers and 3D cultures.

Conclusion: We have demonstrated that MSCs can be isolated from HFP and UC. HFPSCs showed greater chondrogenic potential and had morphological resemblance with native cartilage. Protein analysis of the supernatants showed extracellular matrix components and regulatory proteins during 3D cultures. Although, classical pro-inflammatory mediators were not identified by LC.MS/MS, more sensitive protein approaches should be used to get more certain results.

Keywords: Articular cartilage, osteoarthritis, cellular therapy, mesenchymal stem cells, umbilical cord, Hoffa fat pad, chondrogenesis, histology, proteomics.

Acknowledgment

The present study was carried out at the Department of Bone and Joint Research Group at Institute of Clinical Medicine, University of Tromsø The Arctic University of Norway.

First and foremost, I would like to express my deepest gratitude to my research supervisor Professor Inigo Zubiavrre Martinez. This thesis would not have been possible without the tremendous guidance and support you have provided me. I will always remember your sincere help and crucial contribution. I am also grateful to my co-supervisor Professor Ole Morten Seternes.

I want to express my great appreciation for all the guidance and help I got from Ashraful Islam from the very beginning of my research till the end. You have shared your expertise with me and contributed a great deal to my project. I would also like to acknowledge the support I received from engineer Kirsti Rønne and Dr. Ann Kristin Hansen. Thank you for always willing to help. You have all created great working environment and I am grateful for that.

I want to express my deepest and heartfelt gratitude and respect to Lars Småbrekke for his help when I most needed it. I would like to thank Jack-Ansgar Bruun for the mass spectrometric analysis.

Finally, I would love to thank my parents for their endless love and support. You have always encouraged me to be the best version of myself and you have been there for me from my early years throughout my lifetime. I am forever thankful and indebted to you. All my precious siblings and loving friends, thank you for supporting and believing in me. I love you all.

Jerusalem Yonas Hambissa

May 2015

List of figures

List of tables

Abbreviation

1,9 –DMB	1,9 -Dimethylmethylene blue
ACI	Autologous chondrocyte implantation
ACI	Autologous chondrocyte implantation.
ADSC	Adipose derived stem cells.
ASC	Adult stem cells.
Beta-ME	Beta-mercaptoethanol
bFGF	basic fibroblast growth factor
BMP2	Bone Morphogenetic Proteins
CDC	centers of disease control and prevention
cPD	Cumulative population doubling level
CS	Chondroitin sulfate
DMEM-	Dulbecco's Modified Eagel Medium.
DMSO	Dimethyl sulfoxide
ECM	Extracellular matrix
ESC	Embryonic stem cell
FBS	Fetal Bovine Serum
GAG	Glycosaminoglycan
HES	Hydroxyethyl starch
HFP	Hoffa Fat Pad
HFPSC	Hoffa fat pad stem cell.
HPLC	high performance liquid chromatography
ICRS	International cartilage repair society

IGF-1	Insulin-like growth factor -1
IHC	Immunohistochemistry
ITS	Insulin, Transferrin and selenite.
JIA	Juvenile Idiopathic Arthritis.
KS	Keratin sulfate
LC	MS- Liquid chromatography-mass spectrometry
LC	MS/MS – Liquid Chromatography Tandem-mass Spectrometry
LP	Link protein
MMP	Matrix Metalloproteinase
MSC	Mesenchymal stem cell.
MSC	Mesenchymal Stem Cells
OA	Osteoarthritis
P/S	Penicillin and Streptomycin.
PBS	Phosphate Buffered Saline.
PG	Proteoglycan
Poly-HEMA	Poly-2-hydroxyethyl methacrylate
SDS	Sodium Dodecyl Sulfate
TGF-β1	Transforming Growth Factor- β1
TGF-β3	Transforming Growth Factor- β3
UC	Umbilical Cord
UC-MSC	Umbilical cord derived mesenchymal stem cells
UNN	University hospital in Northern Norway

Table of content

1 INTRODUCTION

1.1 Relevance of the study

Despite the fact that technology, research and knowledge for diseases and their treatment have progressed, some disorders are still unmanageable. Arthritic diseases are very common chronic inflammatory diseases and still represent a major clinical problem in both the developed and developing world. Degenerative joint diseases compress a complex family of musculoskeletal disorders, and are characterized by many different conditions where joints, cartilage, bones and other connective tissues are damaged. This causes swelling, stiffness, loss of motion in joints and severe pain. Even though arthritis is common among older adults (with prevalence in women), it also occurs in children, a condition known as Juvenile Idiopathic Arthritis (JIA [1]. Within degenerative joint disorders, osteoarthritis (OA) and rheumatoid arthritis (RA) represent the most frequent forms of arthritic diseases. According to centers of disease control and prevention (CDC), in 2001-2012, 52.5 million adults in USA have clinically-diagnosed arthritis and it is estimated that the number will increase to 67 million by the year 2030 (http://www.cdc.gov/arthritis/data_statistics.htm). In Norway, a study on based on the Oslo Rheumatoid Arthritis Register (ORAR) reported that RA affects 0.5% of the population [2].

1.2 Synovial joint

The place where two bones are connected together is called joint. There are three types of joints in the human body:

- Immovable joints (Syntharthroses):- for instance connection of teeth to the skull.
- Movable mixed articulations (Amphiarthroses), a joint that allows a slight amount of movement.
- The movable joints (Diarthroses) also called synovial joints.

Synovial joints include joints in the elbow, shoulder, hip and knee, providing the body movement necessary for daily function. The synovial joint is made up of articular cartilage, subchondral bone, ligaments, synovial fluid, synovial membrane and the capsule that embraces the different tissues types. The tendons and ligaments hold the elements in place and the

synovial fluid nourishes and lubricates the surfaces of the tissues. The different tissue types have different tasks and work together making up an organ, the synovial joint [3].

1.3 Articular Cartilage

Articular Cartilage is a connective tissue that covers the ends of long bones within the synovial joints and has two important functions: it provides a frictionless surface for smooth pain-free articulation and ii) limits the stress applied to subchondral bone during joint movements by absorbing the energy of the mechanical loading. The tissue's unique structure enables it to undergo deformation when external stress is applied, and restore its original shape when removed. The other unique nature of articular cartilage tissue is that it is avascular, aneural and without lymphatic vessels and it is composed of a single cell type, the chondrocyte. The dense and abundant extracellular matrix (ECM) present in cartilage tissue facilitates the diffusion of nutrients and waste material in cartilage [4-6].

Articular cartilage has four horizontal layers or zones based on their differences in chondrocyte morphology, collagen fiber orientation and glycosaminoglycan concentration. They are termed superficial layer, transitional (or intermediate) zone, radial zone (deep zone) and calcified cartilage layer (Figure 3.1).

1) Superficial zone, which is nearest to the articular surface, consists of flattened, discoid cells lying between collagen fibers oriented parallel to the articular surface. The collagen fibers are uniform, densely packed and lies predominantly in one direction. The proteoglycan content is low while water content is highest in this zone.
2) The transitional layer has slightly bigger and round shaped chondrocytes. In this zone, the proteoglycan content is higher and collagen fibers are randomly arranged.
3) The radial zone, also known has the deep zone, is the broadest layer and has fairly larger chondrocytes grouped in columns. This has the lowest cell volume but highest proteoglycan content. The water content is low and the collagens are randomly arranged.
4) Tidemark separates the radial zone from the underlying layer of calcified zone where the cartilage and bone tissue meets. [7-11].

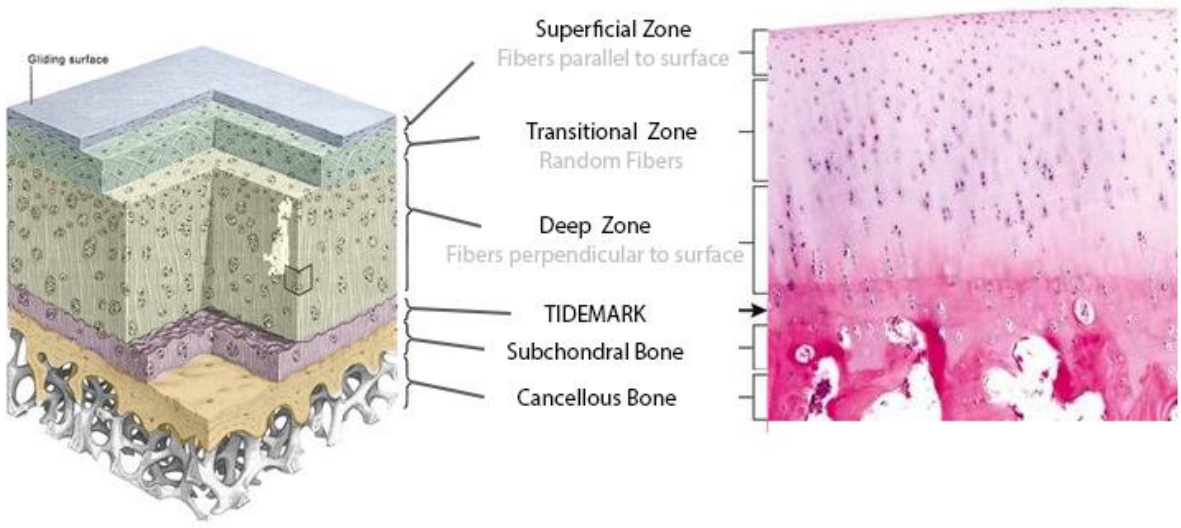

Figure 1. The four zones of articular cartilage with depth-dependent orientation. Superficial zone is the thinnest while the deep zone is the broadest layer. Image adapted from Orthobullets.com.

The chondrocytes in cartilage synthesize mainly collagen type II, aggrecans and some specific extracellular matrix components [6]. These matrix proteins are the main components and are therefore major phenotypic markers to articular cartilage. The adult hyaline cartilage is principally composed of 65-85% water, 12-24% collagen, 3-6% GAG, and 16,000-90,000 chondrocytes per mg tissue wet weight.[12]. Weight-bearing and less-weight-bearing regions show differences in size and number of chondrocytes in the different zones of cartilage. Cell density is highest at the articular surface and decreases in each zone moving closer to the tidemark. Similarly, the amount of collagen and water is highest at in the superficial zone and decreases with increasing distance from the articular surface. In contrast, the proteoglycan content is low in the superficial zone and high in the deep zone [7, 10].

1.3.1 Chondrocytes

The chondrocytes, being the only cell type in articular cartilage, are the functional units of the articular cartilage and responsible for the synthesis, degradation and maintenance of the ECM. They synthesize and maintain the ECM components in a highly ordered structure. The immediate extracellular surrounding the chondrocyte membrane is called Lacunae or

pericellular matrix[5]. The pericellular matrix makes a capsule forming a protective 'cacoon' around chondrocytes, providing a mechanical protection for the cell. The structure formed by chondrocytes and pericellular matrix is also called "chondron". Chondrocytes do not have cell-cell contact and communicate via ECM using mechanical, electrical and physico-chemical signals [5, 9, 13]. Because articular cartilage is avascular, chondrocytes operate at low oxygen tension using glycolysis for their energy source. The oxygen tension can vary from 10% at the surface to <1% in the deep layers [6]. Chondrocytes get their nutrition, including oxygen, from synovial fluid by diffusion system, both through synovial membrane and ECM [10]. The double membrane diffusion system is how they convey metabolites and waste materials as well. Chondrocytes are mainly round-shaped but their morphology and metabolic activity differs in the different zones of the cartilage as mentioned previously.

1.3.2 Extracellular Matrix (ECM)

Extracellular matrix is composed of tissue fluid, structural macromolecules and other non-structural proteins embedded in the fibrillary net, and confers the mechanical properties of the cartilage. Chondrocytes in lacunae [9], are anchored to the ECM by transmembrane proteins such as ancorin and integrins [14, 15]. Loss of proteoglycans in the pericellular matrix is associated with OA.[13]. The matrix surrounding the chondron is called territorial and adjacent to interterritorial matrix, which is present throughout the cartilage. These compartments function synergistically to withstand stress applied under daily body movement [11].

Collagen molecules are composed of approximately 300 nm of triple helix. Although approximately 90% of the collagens in adult cartilage tissue is collagen type II, articular cartilage contains other types of collagen such as type I, III, V, IX, X , XI and a small amount of type VI collagen [16, 17]. Collagens in pericellular matrix are fine fibrils that forms a basket-like network around the chondrocyte cells. In territorial matrix, the collagens are thicker and found in bundles, while the interterritorial matrix consists of dense and closely packed collagen fibers [11]. Collagen type II has the function of providing tensile strength to the articular cartilage [18] as well as anchoring chondrocytes to the ECM [14]. This randomly formed network entraps proteoglycans and glycoproteins in ECM. Type IX collagens are found on the surface of collagen type II at intersection of the fibrils. This collagen is also a proteoglycan and has a sulfate chain covalently linked in NC3 domain of the α2(IX) chain. It contributes to

stabilize the collagen network of ECM by potentially crosslinking the fibrils of collagen type II to each other or other ECM components [19-21]. Collagen XI contributes in regulation of fibril size and is indicated to be linked to α1(II), but mainly to each other [22, 23].

Proteoglycan (PG) is composed of a glycosaminoglycan (GAG), such as chondroitin sulfate (CS) and keratin sulfate (KS), covalently attached to a protein. Aggrecan is a major PG in articular cartilage and is contained within the 3-dimentional fibrous collagen network [24]. Hyaluronic acid, which is one of the GAGs in the ECM, is anchored to collagen fibrils and to link protein (LP) giving stabilization to ECM. [24-26]. The main function of PGs is providing comprehensive stiffness, which arises as physical consequence of their hydrophilic property. The negative charge on KS and CS creates a high osmotic pressure that draw water into the ECM, causing the ECM to expand and swell. When load is applied, water is forced to flow from the matrix, leaving the concentration of aggrecans and charge density to increase. This imbalance causes the aggregans to repeal each other. Aggregans and collagen fibers form a strong porous and permeable solid matrix that is stiff. The load on ECM makes the pore to reduce in size, increasing the resistance of redistribution of water molecules. This mechanism protects and stiffens the cartilage giving the cushion needed to reduce and distribute stress on subchondral bones [8, 26, 27].

The interaction between PGs and collagen maintains the matrix hydrated, and with ECM composition in perfect balance, provides a normal functioning cartilage. An imbalance created by denaturation of collage type II [28] and PGs [29] affects the articular cartilage negatively and is seen in OA.

1.4 Articular cartilage disorders

Articular cartilage is an essential part of the skeletal system for daily function. Its low regenerative ability makes articular cartilage lesions a serious damage, leading to loss of tissue and degenerative joint disease. International cartilage repair society (ICRS) has provided a standard scoring system for macroscopic evaluation of cartilage repair defects [30]. Some of the diseases that can affect cartilage are Achondroplasia, Relapsing polychondritis and Arthritis. Achondroplasia, a condition known to cause dwarfism, occurs when the proliferation of chondrocytes in the cartilage fail [31, 32]. Replapsing polychondritis is a rare chronic disease

that is caused by inflammation of cartilaginous tissues. It occurs with varying degrees of severity and can lead to a permanent destruction of the involved structure [33]. Focal cartilage injuries such as traumatic sport-accidents, wear and tear occurring over time can degenerate cartilage tissue that can develop into arthritis with time.

1.4.1 Osteoarthritis

Osteoarthritis (OA) is considered one of the most common forms of arthritis, a major cause of physical disability amongst non-hospitalized adults, particularly in the aging population. Limitation in their daily activity due to their discomfort is a burden not only for the sick individuals, but also has an important impact on the society. In many people, this chronic and progressive disease affects often their lifestyle, frequently resulting in depression and feelings of helplessness (http://www.niams.nih.gov/Health_Info/Osteoarthritis/default.asp#3). Because of their high prevalence, the associated cost of treatment, loss of productivity and sick leaves are causing enormous costs for health and social care system [34-36].

Osteoarthritis is a multifactorial disease where both genetic and environmental factors play major roles in its etiology. Proinflammatory cytokines and mediators, produced by the synovium and chondrocytes, and their interactions with mechanical stress play an important role in initiation and progression of OA [37]. History of injury and joint overload resulting in deterioration of the joint increases the relative risk of development and progression of OA [35, 38, 39]. OA is not just a degeneration of the articular cartilage, but a disease that affects the whole synovial joint organ. It is characterized by loss of articular cartilage, mild inflammation of synovial tissue [37, 44] and changes in subchondral bone [45] resulting in increased friction, redness, joint swelling and pain. OA usually affects large weight-bearing joints, such as hip and knee. When cartilage is damaged, the chondrocytes near by the defect initiate a repairing process by up-regulating the matrix synthesis and turnover [46]. The continuous mechanical load and the permanent inflammatory response interferes with the delicately balanced catabolism and anabolism of the matrix, leading to production of the proteolytic enzymes. Increased synthesis of matrix metalloproteinases (MMPs) and aggrecanases leads to cell death and decreased synthesis of ECM. This makes the cartilage weak to withstand mechanical stress. The molecular fragments produced initiate synovitis[47], and in parallel the inflamed synovium produces pro-inflammatory cytokines [37, 48] that enhance the excess production of catabolic

enzymes. This vicious cycle goes on promoting joint degradation and inflammation, resulting in chronic joint pain and dysfunction. [47-49]. Articular cartilage possesses a very little potential of self-repair. Additionally, since it is an avascular and anerural tissue, the clinical signs of the damage do not appear before other vacuolated tissues are involved and the disease has progressed.

Age is a strong risk factor and predictor of OA development with high prevalence during aging [39, 40]. A study done on hand OA, Heberden's nodes, in 1943 suggested the involvement of a single autosomal gen that is dominant in females [41]. Since then, other studies have focused on genetic background in OA. Twin studies conducted in London, UK, has reported that the genetic influence in OA is strong and noteworthy[42]. Obesity [43] , osteoporosis and female gender are other acknowledged risk factors of OA. Women are more likely to develop OA than men, especially OA of the knee[39].

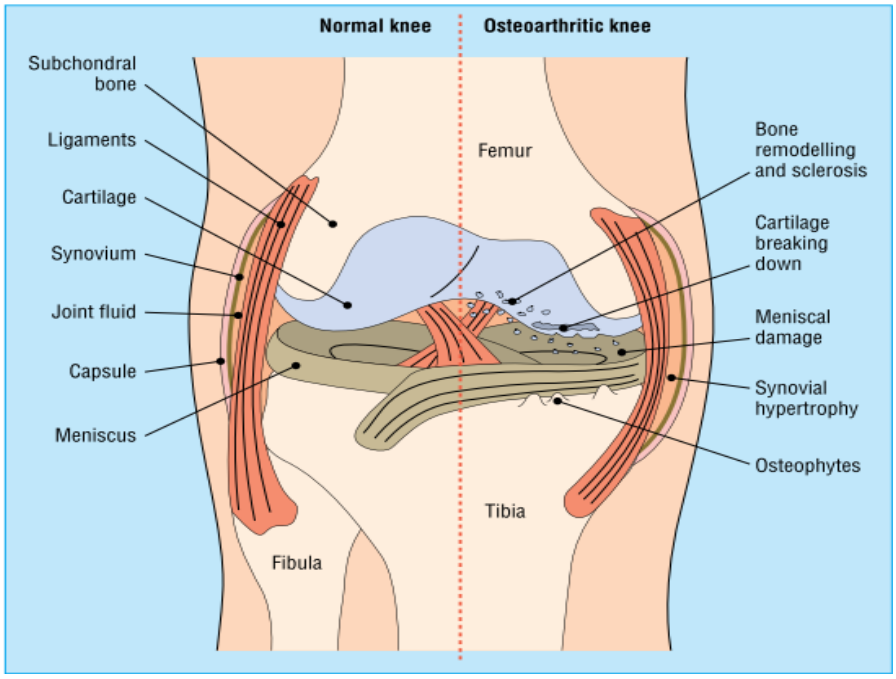

Figure 2. Changes that occur in OA synovial joint. In OA, the whole joint is affected resulting, in amongst many, joint inflammation, stiffness and severe pain. Image adapted from [50]

1.5 Stem Cells

Stem cells are undifferentiated multipotent cells with the capacity of unlimited self-renewal and long-term viability. After cell division, the daughter cells can divide to form more precursor cells or to cells that are functionally specialized matured cells. There are various types of stem cells based on their differentiation capacity. Stem cells from Zygote, fertilized egg cells, are **totipotent** cells that are capable of differentiating to all kinds of cell that make up the embryo and cells necessary for the development of all tissues and organs in adult body, including the placenta and umbilical cord. **Pluripotent** cells are isolated from the embryo and can give rise to all kinds of cells, except the umbilical cord and placenta. These embryonic stem cells (ESCs) have been isolated from mouse embryo by Evans and Kaufman in 1981 and eventually from human blastocysts [50].

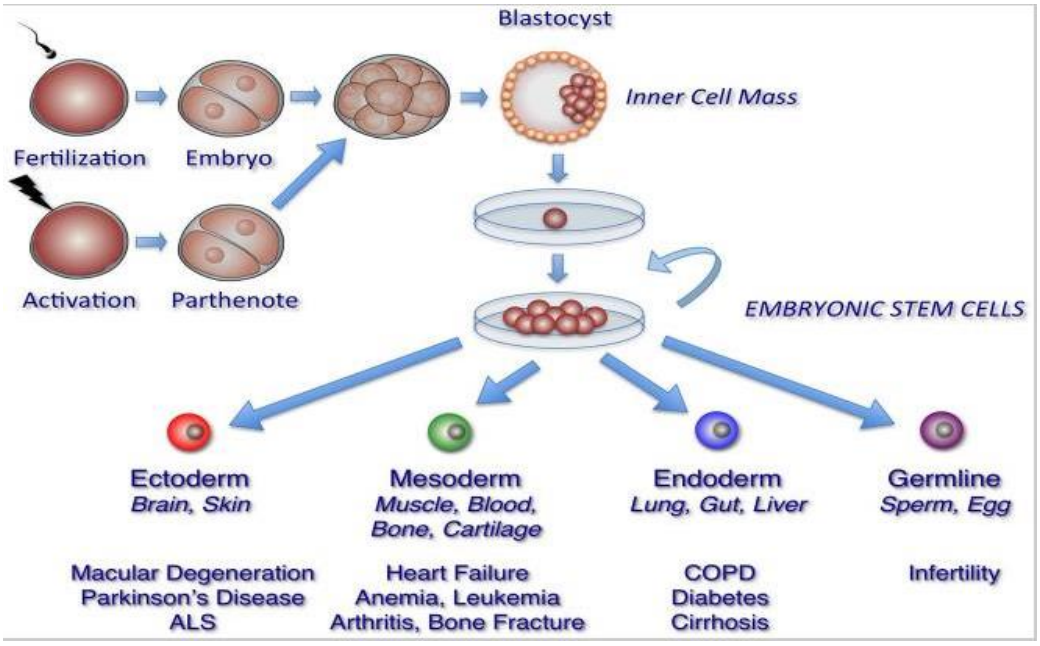

Figure 3 Pluripotent cells can be isolated from the inner cell mass of blastocyst. They give rise to all organ cells in human adult body (Image adapted from [52]).

Adult organisms also contain progenitor stem cells deposited in various organs, such as bone marrow, synovial membrane, liver, intestine, fat and skin. These adult stem cells (ASCs) remain undifferentiated until initiated in response to a signal. Some cells proliferate to produce

precursor cells to maintain the stem cell pool, while others divide to generate and differentiate into tissue specific cells. These cells are responsible for regenerating and replenishing cells after trauma or disease and maintain tissue homeostasis throughout the life. A very good example for this process is renewal of circulating blood cells and replenishment of skin tissue after a trauma. ASC have more restricted differentiation potential than ESCs and if the source is tissue of mesenchymal origin they are called mesenchymal stem cells (MSCs) [51, 52].

1.5.1 Mesenchymal stem cells

Mesenchymal stem cells are adult stem cells that have **multipotent** differentiation potential and have high replicative capacity. Their progeny are capable of differentiating into multiple lineages like osteoblast, adipocytes, chondrocytes, endothelial and muscle cells. [51-54]. Mesenchymal stem cells can be isolated from various human tissues, including adult bone marrow, teeth [55], adipose tissue, synovial membrane and perinatal tissue like placenta[56] and umbilical cord [57, 58].

The Mesenchymal and Tissue Stem cell committee of the International society for cellular therapy has proposed universally accepted minimal of three criteria to define human MSC. The purpose is to provide the same criteria and protocol to work with for all laboratories around the world [59, 60].

The three criteria are:-

1) The cells need to adhere to the tissue culture flask when kept in standard culture conditions and form colonies (**colony-forming potential**).
2) They must express antigens such as endoglin (CD105), ecto 5' nucleotidase (CD73) and Thy-1 (CD90) but also lack expression of hematopoietic and other stem cells markers such as CD45. CD34, CD14 or CD11b, CD79α or CD19 and HLA-DR. (**specific surface markers phenotype**).
3) When maintained under specific *in vitro* tissue culture-differentiating conditions, these cells must be able to differentiate giving rise to osteoblasts, adipocytes and chondrocytes. (**multi-lineage differentiation potential human MSC**)

1.5.1.1 Hoffa Fat Pad stem Cells

Adipose tissue is a source of MSCs that have high proliferation rate and the potential to differentiate toward the osteogenic, adipogenic, myogenic, and chondrogenic lineages. [61-65]. Their great proliferative capacity [64] is not the only advantage adipose derived stem cells (ASCs) have. These cells can be acquired in larger quantities with a far less invasive procedure than bone marrow derived stem cells. Hoffa fat pad stem cells (HFPSCs) have proven to share immunosuppressive properties with bone marrow mesenchymal stem cells (BM-MSCs). They display immunomodulatory effect through suppression of mixed lymphocyte reaction and their proliferative response to mitogens in a cell concentration-dependent manner. Cell surface molecules expressed by HFPSCs exhibit costimulatory effect, and help boost the immunosuppression activity [66, 67]. HFPSCs provide abundant, safe and effective source of MSC, and hold promise for stem cell research and range of therapeutic applications [68].

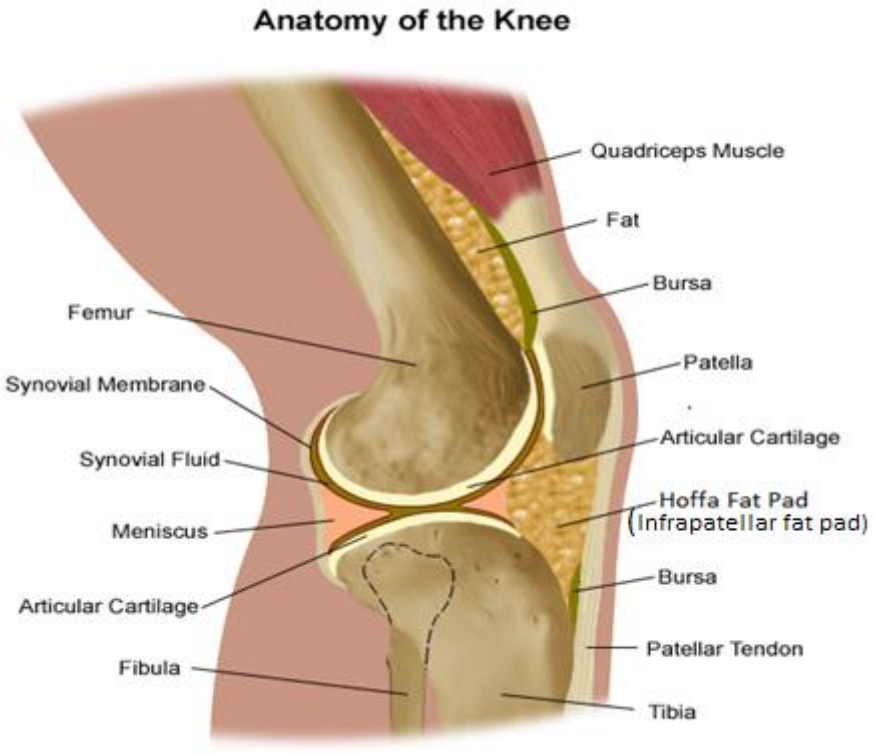

Figure 4. Anatomy of the knee. Hoffa fat pad tissue is located below the patella. (Image adapted from Johns Hopkins medicine with a little modification.) http://www.hopkinsmedicine.org/

1.5.1.2 Umbilical Cord Derived Mesenchymal Stem Cells (UC-MSCs)

Umbilical Cord is a very rich source of mesenchymal stem cells. These stem cells meet the minimal criteria set by the mesenchymal and tissue stem cell committee of the International society for cellular therapy. They are adherent to plastic, have a multi differentiation potential and a great self-renewal rate. They possess the ability to differentiate into chondrogeneic, adipogeneic and osteogeneic lineage in vitro [58, 69]. They also differentiate into cardiomyocytes and neuron specific cells [70, 71] and possess immunosuppressive potential [72]. Human umbilical cord consists of one vain and two arteries surrounded by a connective tissue called Wharton's jelly [69]. Human umbilical cord-derived mesenchymal stem cells (UC-MSCs) can be isolated by digesting the complete cord (mixed cord stem cells) or from the different regions of the cord. Isolation of stem cells from specific cord regions, such as vein [70], Wharton's jelly [71], cord perivascular [73] and subendothelial layer of cord [74] have been successful. Enzymatic digestion of the complete cord provides MSCs that are as good as cells isolated from the individual cord regions from the same cord. Therefore, one does not need to put excess time in dissection of the cord into different regions in isolation of MSCs [69].

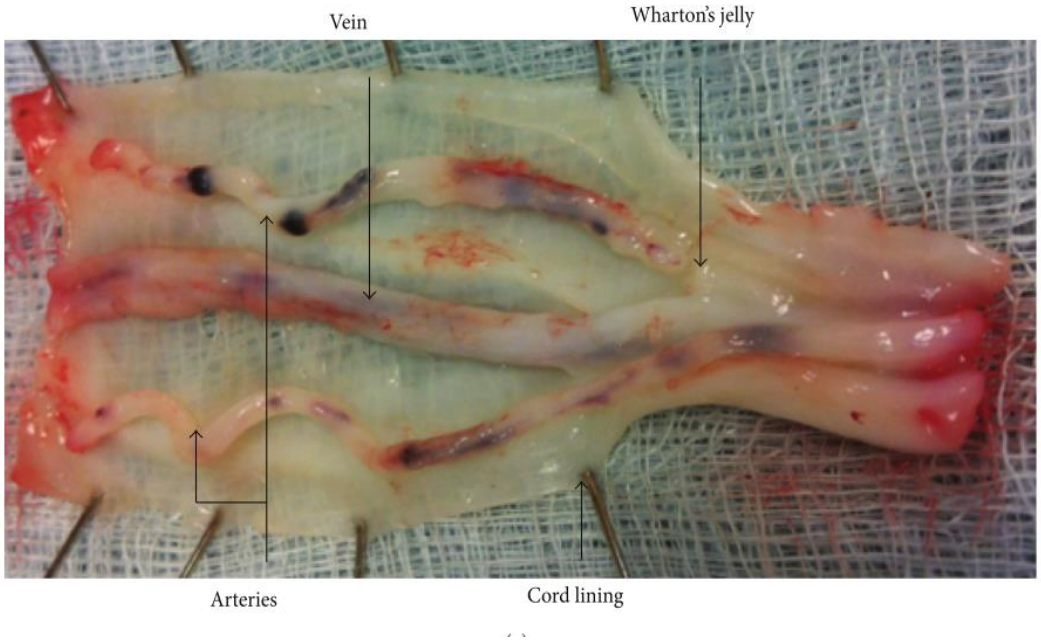

Figure 5. The different regions of human umbilical cord. Isolation of MSCs is possible from the specific regions as well as the whole cord by enzymatic digestion (Image modified from [72])

1.5.1.3 Anti-inflammatory and immunomodulatory properties of MSCs

In addition to being multipotent and highly proliferative, MSCs have immunomodulatory properties. They have a dose-dependent inhibitory effect on activated T-lymphocytes (T-cells) stimulated by different mechanisms. Proliferation of T-cells activated by CD34 and CD 28 antibodies as well as alloantigen and mitogens are inhibited by MSCs. The effect has no immunological restriction and is evident when evaluated with both autologous and allogeneic MSCs [75-77]. While some investigators have reported that direct cell-cell contact is required [78], others have demonstrated that the suppression is due to soluble molecule(s). This is because separation of the two cells by a semi permeable membrane does not abrogate the suppression effect [76, 77]. Dendritic cells (DC) are antigen presenting cells and are important in initiation of the adaptive immune response. MSCs modulate immune response by affecting both the generation and function of DCs. MSCs have a dose-dependent suppression affecting the development and maturation of the DCs. Production of costimulatory signals and MHC class II are reduce and consequently, the capacity of DC to stimulate T-cells is suppressed [79]. Similar to DCs and T-cells, the effect of MSCs on natural killer cells (NK) is dose-dependent. The proliferation of NK cells and cytokine secretion are suppressed by MSCs through cell-cell contact and soluble factors. Interestingly, MSCs are susceptible to lysis by activated NK cells [80]. The immunomodulatory property of MSCs has been put to in vivo test in a phase II study, where safety and efficacy of MSCs for severe graft-versus-host disease (GVHD) treatment has been assessed. More than half of the patients responded well to the treatment and were alive at 2 years [81]. This study, along with others [77, 82], showed a potent immunosuppressive effect with an encouraging result.

1.5.1.4 The use of mesenchymal Stem Cells in biological repair of cartilage

Today, various techniques are used in articular cartilage damage repair. Microfracture, mosaicplasty and Autologous Chondrocyte Implantation (ACI) are some of the widely used methods[83, 84] Harvesting cells from the same patient to reconstruct cartilage *in situ* that is injected into the cartilage defect has been used for over two decades. ACI was first used clinically in Sweden in 1987. In 1994, ACT was performed on 23 people with deep cartilage defect in the knee in Gotheburg, Sweden, at Sahlgrenska University Hospital [85]. Since then, this treatment has been performed numerous times. Although the treatments mentioned above

have shown encouraging short-time clinical outcomes, they are associated to drawbacks such as donor site morbidity, limited availability, unknown or variable long-term durability [83, 86, 87].

Mesenchymal stem cells are able to differentiate into diverse mesenchymal phenotypes, including chondrogenic lineage. Their unlimited self-renewal ability makes them a perfect target for cellular therapy. Stem cell sources such as adipose tissue and umbilical cord are abundant and require minimal invasion. This helps to overcome challenges such as limited availability and donor site morbidity. In regenerative medicine, MSCs are differentiated in a specific lineage pathway in a controlled manner, to effect repair of damaged organ. The chondrogenesis of MSCs have been explored both in small and large animals with cartilage defect. Undifferentiated MSCs have been implanted in experimentally created cartilage defect in rabbits using different delivery methods and scaffolds. The outcome of the studies showed MSCs treatment had superior healing compared with untreated cartilage defects [88, 89]. Larger animals have also been used as a closer system to human physiological condition [90]. Merino sheep treated with chondrogenically predifferentiated ovine MSC implanted in hydrogel construct, showed cartilage development with morphologic characteristics of hyaline cartilage [90]. The integration of the MSCs with the subchondral bone and adjacent cartilage has also been observed on a rabbit model [89]. Although clinical studies on humans are very few, some studies have shown encouraging results. Autologous bone marrow MSCs were expanded in vitro and implanted in defect area in a scaffold. The study population was 5 patients, and 3 of them got complete defect fill and surface congruity with native cartilage [91]. The application of MSCs in cartilage repair has developed rapidly and is being used in clinical trials. Within the many conducted clinical trials, in a recent study treatment of knee OA with autologous expanded bone marrow MSCs in 12 patients has provided supportive evidence that stem cell treatment has a bright future in cartilage repair therapy.

2 AIMS OF THE STUDY

The current treatment available for osteoarthritis has not been successful in restoring the natural cartilage integrity hitherto. HFPSCs and UCSCs can be harvested safely, effectively and in abundant quantities, making them ideal for cellular therapy. Despite previous efforts from other laboratories on using these cell sources for the repair of articular cartilage, the intrinsic chondrogenic capacity of these cells is not completely understood. The scientific community still have not reached a consensus on which cell source is the most suitable to attempt cartilage repair. Additionally, although it has been suggested that these stem cells possess immune-suppressive abilities, it is unknown if such phenotype is retained after differentiation towards specialized tissue cells.

The purpose of this project is to explore and compare the intrinsic chondrogenic abilities of HFPSC and UCSC in scaffold-free 3D models, and to study changes in the cell phenotypes before and after differentiation by secretomics. To achieve this, the work plan is divided in four major objectives:

1. Establish protocols for the isolation and characterization of stem cells from Hoffa-fat-pad and umbilical cords.
2. Establish protocols for in vitro chondrogenic differentiation using scaffold-free 3D models.
3. Study degree of cartilage differentiation in 3D constructs.
4. Study changes in cellular phenotype during cell differentiation by analyzing the secretome, emphasizing on potential inflammatory and immunogenic factors expressed by the cells.

3 MATERIALS AND METHODS

3.1 Materials and Reagents

Table 1. List of materials and reagents used in the research.

24-well ultra-low attachment surface plate	**Catalog# 734-1584**	**Corning lifeScience, USA**
4% Paraformaldehyde	Kindly provided by department of Pathology at University hospital in Northern Norway (UNN), Tromsø	
96-conical bottom well plates	Catalog# 249935	ThermoScientific, Danmanrk
Agarose	Catalog# V3121	Promega corportation, USA
Alcian Blue 8GX	Catalog# A9186	Sigma-Aldrich, Germany
Alcian blue staining	Catalog# A5268	
Aluminum sulfate	Catalog# A7523	
Basic fibroblast growth factor (bFGF)	Catalog# 100-18C	Peprotech, UK
Beta-mercaptoethanol	Catalog# M6250	Sigma-Aldrich, Germany
BD stemflow hMSC analysis kit	Catalog#562245	Bd Biosciences, USA
Bio-Rad DC protein assay kit	Catalog#5000112	Bio-Rad, Norge
Blyscan sulfated GAG assay	Catalog# B1000	Biocolor, UK
Bone Morphogenetic protein 2 (BMP2)	Catalog#120-02C	Peprotech, UK
Cell strainer 70 µm	Catalog# 431751.	Corning lifeScience, USA,
Collagenase XI	Catalog# C9407	Signma-aldrich, Germany
Coomassie blue	Catalog# LC6065	Sartorius, Germany
Dexamethasone	Catalog# 364897	Galen, Germany
Dimethyl Sulfoxide (DMSO)	Catalog# WAK- DMS-10	Wak-chemie Medical GMBH, Germany

Table 1 Continued

Dulbecco's modified eagle's medium (DMEM)	Catalog# D5796	Signma-aldrich, Germany
Enzyme-free dissociation solution	Catalog# S-014-B	Millipore, USA
Ethanol	Catalog# 32221	Sigma-Aldrich, Germany
Fetal Bovine Serum (FBS)	Catalog# 50615	Millipore, USA
Glacial Acetic Acid	Catalog# 27225	Riedel-de Haen
Haematoxylin	Catalog# RBA-421300A	Chemi-teknikk, Norway
Insuline-transferrin-Selenium (ITS)	Catalog# 392-2505	Peprotech, Uk
Insulin-like growth factors (IGF-1)	Catalog#100-11	Peprotech, UK
L- Ascorbic acid	Catalog# 103033E	Analar BDH laboratory, UK
L-cstein hydrochloride monohydrate	Catalog# C6852	Sigma-Aldrich, Germany
Non-vented culture flasks 25 cm^2	Catalog# 156340	ThermoScientific, Danmanrk
Nuclear Fast Red	Catalog# N3020	Sigma-Aldrich, Germany
Nunc cell culture flask 175 cm^2	Catalog# 159910	ThermoScientific, Danmanrk
Nunc cell culture flask 75 cm^2	Catalog#156499	ThermoScientific, Danmanrk
Papain digestion Enzyme	Catalog# P3125	Sigma-Aldrich, Germany
Penicillin and Streptomycin (P/S)	Catalog# P4333	Sigma-Aldrich, Germany
phosphate buffered saline (PBS)	Catalog# D8537	Signma-aldrich, Germany
Polyhema	Catalog# P3932	Signma-aldrich, Germany
SILAC DMEM heavy	Catalog# 89985	Thermo Scientific
SILAC DMEM light	Catalog# 89985	Thermo Scientific

Table 1 Continued

Sodium phosphate buffer EDTA	Kindly provided by Ph.D candidate Ashraful Islam at Bone and Joint research group.	
Transforming growth factor β 1 (TGF-β1)	Catalog#100-21C	Peprotech, UK
Table 1 Continued		
Transforming growth factor β 3 (TGF-β3)	Catalog#100-36 F	Peprotech, UK
Trypan Blue solution	Catalog# T8154	Sigma-Aldrich, Germany
Trypsin-EDTA 0,25%	Catalog# T4049	Sigma-Aldrich, Germany
VivaSpin column	Catalog# VS0612	Sartorius, Germany
Xylene	Catalog# 534056	Sigma-Aldrich, Germany

3.1.1 Cell growth medium

In cell culture, basal medium containing antibiotics and ascorbic acid is used for controlled cell growth and differentiation. Penicillin and Streptomycin (P/S) prevent bacterial contamination of the cell culture due to their effective combined action against gram-positive and gram-negative bacteria. Ascorbic acid, in addition to acting as a reducing agent, stimulates MSC proliferation without loss of phenotype and differentiation potency. The effect is dose-dependent, and requires proper amount when supplied to culture medium. Another effect, which is important for the experiment we are conducting, is its ability to increase collagen and GAG production in ECM [92, 93].

Fetal Bovine Serum (FBS) is one of the widely used animal serum in cell culture media for its essential components. It contains embryonic growth promoting factors, hormones, transport proteins, adhesion-promoting and others essential molecules [94]. Serum-free medium containing different growth factors and hormones along with different cytokines are used in 3-dimentional (3D) cell cultures to initiate chondrogenic differentiation.

3.1.1.1 Preparation of serum-containing growth medium

The basal growing medium was prepared by adding a solution containing Penicillin and Streptomycin (P/S) (1%) and ascorbic acid (1%) to a high glucose content Dulbecco's Modified Eagel Medium (DMEM). In addition, basic fibroblast growth factor (bFGF) (50ng/ml) and FBS (10%) were added to the basal medium to promote growth during cell expansion. Basal medium is warmed in 37 °C heating cabinet prior to use.

3.1.1.2 Preparation of Chondrogenic medium

The basal growing medium (DMEM supplemented with P/S and ascorbic acid) was used enriched by administration of dexamethasone (1µg/ml) and Insulin-Transferrin-Selenium (ITS) mix (1:1000 stock solution).

To check the best combination of chondrogenic factors, four different media formulations were tested.

1- Basal DMEM + Dexamethasone + ITS + TGF-β1 + BMP-2
2- Basal DMEM + Dexamethasone + ITS + TGF-β1 + IGF-1
3- Basal DMEM + Dexamethasone + ITS + TGF-β3 + BMP-2
4- Basal DMEM + Dexamethasone + ITS + TGF-β3 + IGF-1

Concentration of growth factors:

TGF-β1	10 ng/ml
TGF-β3	10 ng/ml
IGF-1	20 ng/ml
BMP2	100 ng/ml

3.1.2 Solutions and reagents prepared for staining of sections with Alcian blue and Nuclear Fast Red

Alcian blue is basic dye that is soluble in water. It stains carboxylated and sulfated proteoglycans (PG) and GAGs of cartilage blue color. The anionic groups of the substrate is required for intense staining. Therefore, Alcian blue at a low pH (2.5) is used. Counter staining

in nuclear fast red solution stains nuclei and cytoplasm, pink/red and pale pink respectively. [95, 96].

3% Acetic Acid solution:

Glacial Acetic Acid	7.5 ml
Distilled water	242.5 ml

Alcian Blue solution (pH 2.5)

Alcian Blue 8GX	2.5 g
Acetic Acid solution 3%	250 ml
Mix well and adjust pH to 2.5	1 M NaOH

0.1% Nuclear Fast Red, 5% aluminum sulfate solution:

Nuclear Fast Red	0.25 g
Aluminum sulfate	12.5 g
Distilled water	250 ml

Aluminum sulfate was dissolved in water. Nuclear fast red was added and heated slowly to boil and cool. The solution was filtered and a grain of thymol was added as a preservative.

3.1.3 Preparation of 1X SDS running buffer for SDS gel electrophoresis

- Deionized water 950 ml
- 20X NuPAGE MES or MIOPS SDS running buffer 50 ml

3.1.4 Preparation of SILAC Media

SILAC Media with light amino acids contains [U-$^{12}C_6$] L-Lysine and [U-$^{12}C_6$] L-Arginine. SILAC Media with heavy amino acids contains [U-$^{13}C_6$] L-Lysine and [U-$^{13}C_6$] L-Arginine. The basal medium was prepared using SILAC media with ITS, dexamethasone, P/S and ascorbic acid as explained in section 3.1.1.2. Growth factors IGF-1 and bFGF were added. SILAC chondrogenic medium was prepared with combination of TGF-β1 + BMP-2 and TGF-β3 + BMP-2 as explained in section 3.1.1.2.

3.2 Human material

Human specimens were collected from the University hospital in Northern Norway (UNN) under donors informed consent. For Hoffa fat pad, the patients were diagnosed with advanced OA, and were in operation for full joint replacement. In total, we received specimens from six donors, men and women. The mean age was 55, with the youngest 38 and oldest 69 years old.

Umbilical cord were collected right after births occurring at the neonate and women health department at UNN. Even though umbilical cords are medical waist, collection happens after parents' informed consent. In total, five umbilical cords were collected for isolation of cells.

3.3 METHODS

3.3.1 Isolation of cells from various tissues.

Isolation of stem cells from the different tissue specimens received from the University hospital in Northern Norway (UNN), was carried out by mechanical mincing and enzymatic digestion. Because collagen fibers are abundant in connective tissue, the enzyme collagenase was used for rapid degradation of the collagen, and effective release of cells from the tissue. Collagenase type XI is isolated from Clostridium histolyticum, and addition of DMEM neutralizes the activity [97]. In this study, we have isolated stem cells from adipose tissues and human umbilical cord.

3.3.1.1 Isolation of stem cells from Hoffa Fat Pad (HFP)

Hoffa Fat Pad and synovial tissue biopsies were obtained from total knee replacement operations at UNN. Synovial membrane was carefully separated from the Hoffa Fat Pad in the laboratory. The tissues were weighed and minced into small pieces (2 mm^3) using sterile scalpel. Digestion was carried out with Collagenase type XI (1,25mg/ml) on a shaker for 1.5 hour at 37 °C in T-25 non-vented culture flask. The suspensions were centrifuged at 800xg for 10 min, and the pellets were resuspended in 15 ml of DMEM supplemented with FBS (20%) to be planted in 75 cm^2 cell culture flask. Cell cultures were kept in a humidified atmosphere with CO_2 (5%) at 37 °C. Fresh medium containing FBS (10%) was changed once a week and passaged upon reaching 70% confluence.

3.3.1.2 Isolation of Mixed Cord stem cells from Human Umbilical Cords (UC)

Umbilical cords were obtained from births occurring at the neonate and women health department at UNN. The whole cord was washed in sterile phosphate buffered saline (PBS) and cut into approximately 2 cm in length. The pieces were then washed with sterile PBS twice to remove red blood cells. Because of high risk for bacterial contamination, cord fragments were immersed in 90% ethanol for 30 seconds, and then immediately rinsed with sterile PBS. "Clean" cords were minced up in small pieces of 1-1,5 mm^3 and put in non-vented flask on a shaker for 1 hour at 37 °C in Collagenase type XI (1,25mg/ml) for enzymatic digestion. The suspension was centrifuged at 800xg for 10 minutes. The pellet was resuspended in DMEM supplemented with FBS (20 %) and plated in 75 cm^2 cell culture flask. Initial cell attachment and expansion was permitted during 3-4 days, before changing fresh medium containing FBS (10%). Medium was changed every week, and monolayer cell cultures were further expanded using trypsinization upon reaching 70% confluence.

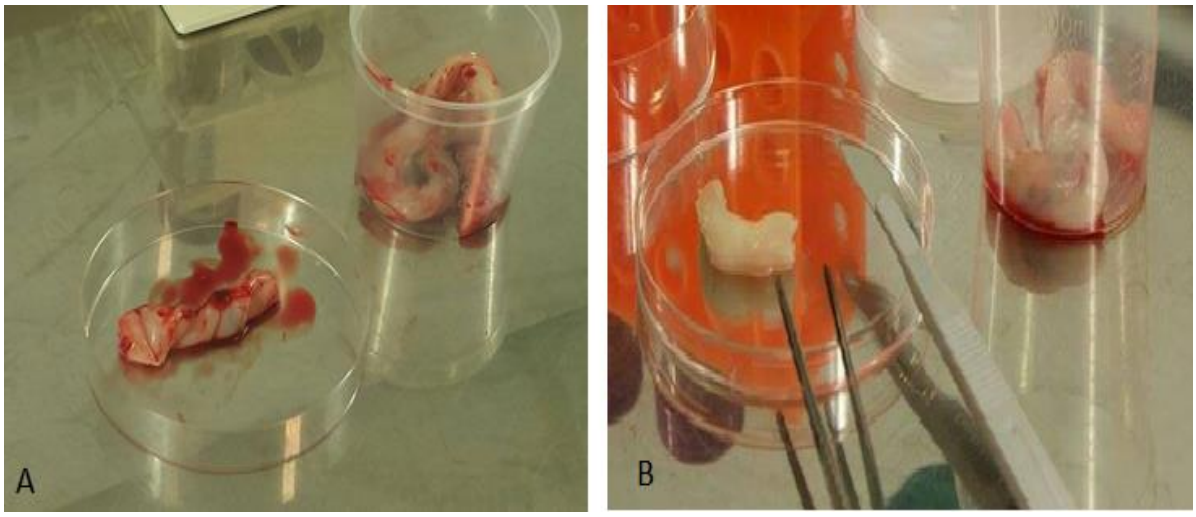

Figure 6. Umbilical cord cut in to a small piece. B) The blood is washed and UC is ready for mincing and enzymatic digestion.

3.3.2 Cell growth rates

The isolated stem cells were seeded in basal medium until 70% confluent. Cells were harvested by trypsinization at semi-confluence. Viable cells were counted using trypan blue exclusion

assay and reseeded in 75 cm^2 culture flask. This procedure was repeated until passage 5. Population doubling was calculated using the following formula: $cPD = \log N / \log 2$,

where N is the cell number of the confluent monolayer divided by the inoculum cell number.

3.3.3 Phenotypic characterization of cells by Flow cytometry

Flow cytometry is a method used to analyze the physical and chemical characteristics of particulate matters, such as cells and cell components. The analyses can be conducted on small particles with size between 0.2 and 150 µm. Fluorescently stained particles are excited by laser, emitting light at varying and specific wavelengths that can be measured to determine the properties of the sample. The wavelength of each particle is processed by a computer connected to the flow cytometry, and presented in histogram, dot plot, density or a contour plot depending on the number of parameters. In this study, immunocytochemical markers for MSCs cell surface antigens were used to identify the phenotype of isolated cells.

When seeded cells were confluent, they were trypsinized and pelleted at 400 x g for 3 minutes at 4°C. The pellet was washed twice with cold stain buffer (FBS), and resuspended to a concentration of 5 x 10^6 cells/ml. The analysis was carried out by Ph.D candidate Ashraful Islam. In addition, CD106, CD166, CD146, CD44 and CD271 were used.

- 100 µL of prepared cell suspension was added to fluorescently tagged markers according to manufacturer's guideline.
- The tubes were incubated in the dark for 30 minutes on ice.
- Cells were washed twice with stain buffer and pelleted at 400 x g for 3 minutes.
- Cells were resuspended in 500 µL of stain buffer.
- Cells were transferred to appropriate flow cytometry tube for analysis.

3.3.4 Freezing and thawing of cells

When seeded cells reached 70% confluence, the cells were washed with room temperature PBS. Enzyme free dissociation solution was added and the flask was kept for 10 min at 37 °C to detach adherent cells. Trypsin-EDTA (0,25%) was then added for a short period of time to finish cell detachment and avoiding formation of cell aggregates. The solution was centrifuged at 800xg for 5 min and the pellet was resuspened for counting viable cells using trypan blue

exclusion in a haemocytometer. The suspension was centrifuged and pellet was resuspened in basal medium containing FBS (20%) and Dimethyl sulfoxide (DMSO) (10%) kept on ice. Cryovials containing $1x10^6$ cells were placed in -20 °C for 1-2 hours then in -80 °C for 24 hours, before storing them in liquid nitrogen tank until use.

To recover the cells, the requested cryovial was removed and quickly thawed. The cell suspension was then transferred to a centrifuge tube containing basal medium. DMSO was removed by centrifugation, and the pellet was resuspended in basal medium containing 10% FBS. The cell suspension was seeded in T-75 culture flask for cell adherence and expansion for further research. During cell expansion, basal medium was kept in heating cabinet prior to use at all times.

3.3.5 Three-Dimensional cell Culture

Research conducted in 2-dimentional cell culture provides a great knowledge about cells, but it is a poor representation of the physiological environment. Creating a third dimension of cell culture, and permitting cells to interact with their surroundings, is necessary to study them in *in vivo-like* condition. There are many different 3D cell culture methods and approaches, such as the hanging-drop method, different scaffolding systems, magnetic levitation, and scaffold-free 3D pellet culture [98-100]. In this study, we use a scaffold-free cell culture, a pellet culture method using 96-well conical-bottom well plates. Poly-2-hydroxyethyl methacrylate (Poly-HEMA) solution was used to coat the conical-bottom wells to prevent cell adhesion to plastic and instead promote cell-cell interaction. This method was developed by Ivasacu and Kubbies [101], and enables rapid generation of 3D spheroids in a time efficient way.

For coating, 1.2 g of Poly-HEMA was dissolved in 100 ml of 96% ETOH using magnetic stirrer at 50 °C. An appropriate volume, approximately 150 µl, was applied to each conical well under a sterile hood. The plates were kept in an incubator at 56 °C overnight, allowing the alcohol to dry out. The coated plates were covered with aluminum foil, and kept in room temperature until use. The plates can be stored and used for up to three months [102]. The plates are placed in heating cabinet with 150 µL sterile PBS for 1-2 hours to wash off remaining Poly-HEMA before use.

When confluent, cells were dissociated and the pellet was suspended in serum-free basal medium. $5x10^4$ cells per 150 µl were transferred into each poly-HEMA coated conical-bottom 96 well culture plates. The plates were centrifuged at 1100xg for 10 min to aggregate cells. The conical well plates were immediately transferred to a humidified atmosphere at 3% CO_2 and 3 % O_2 at 37 °C. After 48 hours, pelleted cells were forming a firm tissue-like construct. At this time of point, pellets were transferred to a 24-well ultra-low attachment surface plate and incubated in a low oxygen atmosphere (CO_2 (3%) and O_2 (3 %) at 37 °C) for 21 days in chondrogenic medium. Half of the chondrogenic medium was changed twice week. After 21 days of incubation in chondrogenic medium, the spheroids were collected and used to assess their chondrogenic differentiation potential by histological and biochemical assays.

3.3.6 Preparation of spheroids for histology.

The 3D cell structures maintained in chondrogenic medium in humidified atmosphere with low oxygen O_2 (3 %) and CO_2 (3%) at 37 °C for 21 days were collected. After washing the spheroids with ice-cold PBS twice, they were fixed in PBS containing 4% paraformaldehyde in refrigerator for 2-24 hours. The fixative was removed and the spheroids were washed with PBS. Haematoxylin was added to color the spheroids before embedding them in a block of 1% agarose-PBS solution and dehydrating it in 50% ethanol. Agarose blocks were delivered to UNN for processing before the group's engineer, Kirsti Rønne, sectioned and stained them with Alcain blue staining.

Staining procedure:

After sectioning the spheroids, the slides were deparaffinized by clearing in xylene twice for 3 minutes. To hydrate the slides, they were first placed in 100% EtOH twice for 2 minutes. Then they were placed in 90% EtOH and 70% EtOH for 2 minutes each before it was hydrated in distilled water for two minutes. The slides were stained with Alcian Blue solution for 30-45 minutes before washing them in running tap water for 2 minutes. Counter staining in nuclear fast red solution was carried out for 3-5 minutes before washing them in running tap water for 1 minute. The slides were rinsed in distilled water for 2 minutes and dehydrated in 70 % EtOH, 95 % EtOH and finally in 100% EtOH for 2 minutes each. Finally, they were cleared in xylene twice for 3 minutes before mounting with resinous mounting medium.

3.3.7 Biochemical measurements of GAGs and DNA from 3D constructs.

70.25 mg L-cysteine hydrochloride was dissolved in 40 ml of sodium phosphate buffer EDTA (PBE). The solution was then filtered sterilized with a 0.22-µm syringe filter. 20 ml sterile PBE-cysteine was transferred to a 50-ml falcon tube. Rubber stopper of the papain enzyme vial was swiped with ethanol to sterilize it. After resuspending, a small amount was removed with sterile 1-ml syringe to a sterile Eppendorf tube. A pipetman was used to add 104 µl papain enzyme to 20 ml PBE-cysteine.

The spheroids were transferred to an Eppendorf tube and washed with PBS twice. 1 ml of papain enzyme solution was added and the Eppendorf tubes were kept on water bath 65 °C for 18-24 hours. The dissolved spheroids were then centrifuged at 1600 G for 10 min to get rid of undissolved debris. The supernatant was transferred to a new Eppendorf tube and stored at -80 °C until use.

3.3.7.1 DNA concentration and normalization

Values for GAGs expression are normalized against amount of total DNA extracted from spheroids. PicoGreen dye has high selectivity for double-stranded DNA (dsDNA) and get 1000-fold intensity of flouresence when bound to dsDNA. The microtubes containing PicoGreen reagent solution must be protected from light in order to avoid photobleaching. Therefore, the procedure of concentration and normalization of DNA must take place in a dark room, in the absence of normal room light. When evaluating the amount of DNA, if the sample reading is outside the standard curve range, a new dilution and reading of sample must be performed [103]. Quant-iT PicoGreen dsDNA assay kit was used and conducted by the manufacturer's instruction.

- 2 µg/mL DNA standard working solution was prepared.
- 6 µL of DNA stock with concentration of 100 µg/mL and 294 µL of TE buffer was mixed well by vortex.
- 10 µL of sample was diluted 10 times with 1X TE buffer to a final sample volume of 100 µL directly in 96-well black microplate. Equal amount, 100 µL, of standards and samples were added in individual well.

- PicoGreen dye was diluted by adding 55 µL of the dye into 11mL of 1X TE buffer.
- 100 µL of PicoGreen was transferred to each well and measured DNA concentration using a microplate reader Tecan Safire. The wavelength excitation at 485 nm was used emitting 535 nm.

3.3.7.2 Quantification of GAG by 1, 9-dimethyl-methylene blue dye essay

The 1, 9-dimethyl-methylene (DMB) is used to measure GAGs and is able to detect as small amount as 2.5 µg/ml. The dye binds to sulfated GAGs such as chondroitin sulfate and keratin sulfate. Papain digestion inhibits the interference that can occur because of bovine serum in the sample. The concentration of GAGs is measured with spectrophotometry based on the metachromasia resulting when DMB stains the sulfated GAGs [104].

Serial dilutions of glycosaminoglycan standard using sterile miliQ water was made with the following concentration: 50, 25, 12.5, 6.25, 3.13, and 1.56 µg/mL. 50 µL of standards and test samples were transferred in 1.5 mL microcentrifuge tubes. 250 µL of Blyscan dye reagent was added and incubated in RT for 30 minutes. After incubation, the samples were centrifuged and the supernatant was discarded. The dye-bound pellet was retained and dissociated with 250 µL dissociation agent per sample to release the color. 200 µL of each sample was transferred to individual wells of a 96 micro plate and measured using CLARIOstar plate reader. Foaming should be avoided to prevent abnormal absorbance readings. Sulfated GAG isolated from the spheroids were measured by CLARIstar microplate reader. Measurement was carried out spectrophotometrically at 655 nm using the Blyscan s-GAG assay kit according to the manufacturer's instructions.

3.3.8 Stable isotope labelling of amino acids in cell culture (SILAC)

SILAC is a technique used for quantification of protein using mass spectrometry. The method relies on the incorporation of amino acids into the newly synthesized proteins when cell cultures are cultivated in medium containing amino acids with substituted stable isotopic nuclei. Analysis of the secretome allows us to quantify and identify the proteins produced by the cells.

3.3.8.1 SILAC labelling of cells in monolayers

Cells were seeded in basal medium containing 10% FBS in T-75 culture flask and maintained for 24 hours in a humidified atmosphere at CO_2 (5%) at 37 °C to promote cell adherence. The culture flasks were marked 'light' and 'heavy'. After 24 hours, the cells were washed three times with DMEM gently. SILAC medium (6ml) of light and heavy containing growth factor were added to the culture flasks accordingly. On The 6th day, the cell cultures were washed extensively with DMEM before incubating in 6 ml of basal SILAC medium. After 5 days of incubating in a humidified atmosphere at CO_2 (5%) at 37 °C, the medium was collected and centrifuged at 4500 rpm for 5 minutes. The supernatant was filtered through sterile 0.22 µm syringe filter. The proteins were concentrated by ultrafiltration in vivaspin column with 5 kDa membrane cutoff by centrifuging at 4500 rpm for 20 minutes. After emptying the container, the concentrator was refilled with 2 ml of PBS and centrifuged again. This washing procedure was repeated three times to remove contaminating micro solutes. The concentrate sample was aspirated and protein concentration was measured.

3.3.8.2 SILAC labelling of cells in 3D cultures.

HFPSCs were plated in high glucose content DMEM 10% FBS containg bFGF. Upon reaching 90% confluence, the cells were dissociated and resuspended in SILAC chondrogenic medium and 150 µl was transferred into each well containing 5 x 10^4 cells. The conical well plate was centrifuged at 1100G for 10 min to form pellets. The newly made spheroids were kept in a humidified atmosphere at low oxygen condition O_2 (3%) and CO_2 (5%) at 37 °C for 48 hours so they can become firm. The spheroids were transferred to a low binding plate where fresh SILAC chondrogenic medium was changed every 4th day. On 16th day, SILAC medium without growth factor was added and collected after 5 days for protein analysis. The protein from the medium was collected and concentrated with the same procedure as explained earlier in section 2.8.3. The spheroids were digested and prepared for DNA analysis as described earlier in section 2.9.

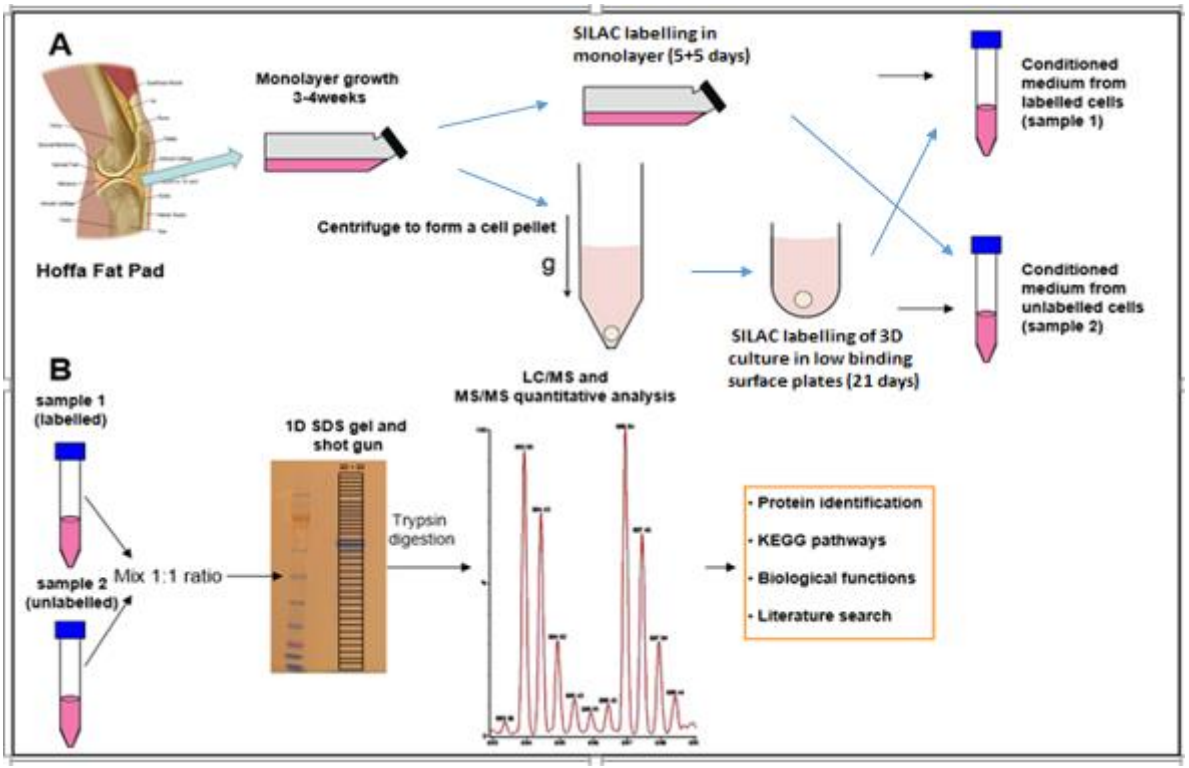

Figure 7. SILAC labelling of cells in 2D and 3D cultures. (A) Specimen of HFP is digested for cell isolation. Isolated cells are seeded in monolayer for expansion and pellets are formated by centrifugation. The pellets are cultured in low-adhesion round-bottom 96-well plate, where SILAC labelling takes place. (B) The supernatant is aspirated and prepared for protein analysis by LC- MS/MS.

3.3.9 Protein quantification assay

Equal amounts of proteins from the different experimental groups must be loaded in gels for comparision, thus total protein amount in samples were determined. Samples were concentrated by ultrafiltration in Vivaspin and then analyzed using Bio-Rad *DC* protein assay kit.

Reagent description

- Reagent A – an alkaline copper tartrate solution
- Reagent B- a dilute Folin reagent
- Reagent S- surfactant solution

1. Standard solution of albumin diluted in sterile PBS with a concentration of 2mg/mL, 1mg/mL, 0,5mg/mL, 0,25mg/mL, 0,125mg/mL, 0,0625mg/mL + BLANK was prepared.
2. 20 µL of reagent S was added to each ml of reagent A.
3. 5 µLof standard and sample was transferred in to the microplate.
4. 25 µL of reagent S+A, made on step 2, was transferred to each well.
5. 200 µL of reagent B was added, mixed well and incubated for 15 minutes.
6. Absorbance was measured at 750 nm on spectrophotometer.

The results acquired from the absorbance was used to prepare samples for SDS gel electrophoresis.

3.3.10 SDS gel electrophoresis

One dimension gel electrophoresis is used to "clean" samples from small molecules and to separate proteins. Proteins are denatured by Sodium Dodecyl Sulfate (SDS) and become charged in their primary structure. Once current is applied, the proteins will migrate from the top, which is negatively charged electrode, towards the bottom, to a positively charged electrode. The separation takes place by means of protein size.

3.3.10.1 Preparation of samples for SDS Gel Electrophoresis

Sample 1: 30 µl of sample was prepared by mixing equal amount of proteins from

1) Light SILAC medium collected from monolayer culture and
2) Heavy SILAC medium collected from 3D structure cells.

Sample 2: 30 µl of sample was prepared by mixing equal amount of proteins from

1) Light SILAC medium collected from 3D structure cells and
2) Heavy SILAC medium collected from monolayer culture

Sample 3: 30 µl of heavy SILAC medium from monolayer culture

Sample 4: 30 µl of sample was prepared from heavy SILAC medium from 3D structure cell culture.

4 µl of NuPAGE LDS sample buffer and 10 µl of reducing agent was added to all samples before heating it at 70 °C for 10 minutes to denature the proteins.

3.3.10.2 Preparation of gel bands for proteomics

The comb at the top and plastic at the bottom of the gel cassette was removed. The gel was rinsed with 1X SDS running buffer before placing it in the electrophoresis unit securely. The upper chamber (inner chamber) was filled up to the top and the lower chamber (outer chamber) half way with 1X SDS running buffer. 500 µl of NuPAGE antioxidant was added to the upper chamber. Samples were loaded and the electrophoresis was run at 200 constant voltage for approximately 15 minutes or until the die front has drifted to the middle of the gel.

Upon completion of electrophoresis, the gel apparatus was taken apart and the gel was removed to be fixed in a solution of: 50% methanol, 40% water and 10% acetic acid for 1 hour on a shaker. For visualization of the proteins, the gel was fixed and stained with Coomassie blue for 1 hour after it was rinsed with unionized water three times. Three protein bands per sample were cut, transferred in to Eppendorf tubes and kept in -80°C. The samples were analyzed with LC-MS for identification of the proteins at the proteomic plat form by Jack- Ansgar Brunn.

3.3.11 Liquid Chromatography Tandem-mass Spectrometry (LC-MS / MS)

Liquid chromatography-mass spectrometry (LC-MS) is an analytic method used to identify, characterize and quantify chemical compounds based on the mass of the particle or/and its fragments in the presence of other molecules. The particles are ionized by variety of methods, such as electron ionization (EI), electrospray ionization (ESI) and atmospheric pressure chemical ionization. The ion is then transported in an environment of high vacuum, typically according to their masse-to-charge (m/z) value. The charged particles are the detected by detectors installed within the high vacuum area at the outlet of the ion, and analyzed when each ion induces an electrical signal. High performance of liquid chromatography (HPLC) was introduced in 1970's, where liquid phase is used. For ionization of the compounds to elute from

the HPLC without production of large amount of gas that can prevent vacuum formation, ionization of the compound must be achieved at atmospheric pressure with selective transfer of ions into the vacuum. This was enabled with electrospray ionization method. Tandem mass spectrometry (MS/MS) has highly specific mass spectrometric delectation and is more advanced technique than LC-MS. It uses two quadrupole mass filters. The first filter selects the m/z of the intact ionized target analyte and filters the other ion species out. All the ions with identical m/z are continuously transferred into the collision cell. These ions collide with either argon or nitrogen gas, fragmenting into characteristic product ions. The ions are transferred into the second quadrupole, where only one selected fragment ion will pass and reach the ion detector. This happens in fractions of seconds and allows multiple analysis at the same time [105].

4 RESULTS

4.1 Cell isolation from tissues and initiation of in vitro culture.

We isolated stem cells from specimens of various tissue types successfully. Cell cultures were maintained in a humidified atmosphere at CO_2 (5%) at 37 °C in high glucose content basal medium. The primary cells isolated from all tissues included in this study contained high number of plastic-adherent and proliferative stem-like cells. Morphological features of MCSCs and HFPSCs were further examined by phase-contrast microscopy. Visual assessment of cultures showed slight differences in cell size and shape. MCSCs are bigger in size and more heterogeneous shape-wise, as seen in figure 1. Of importance, the cells maintained their proliferative and plastic-adherent properties after freezing down and recovering from liquid Nitrogen.

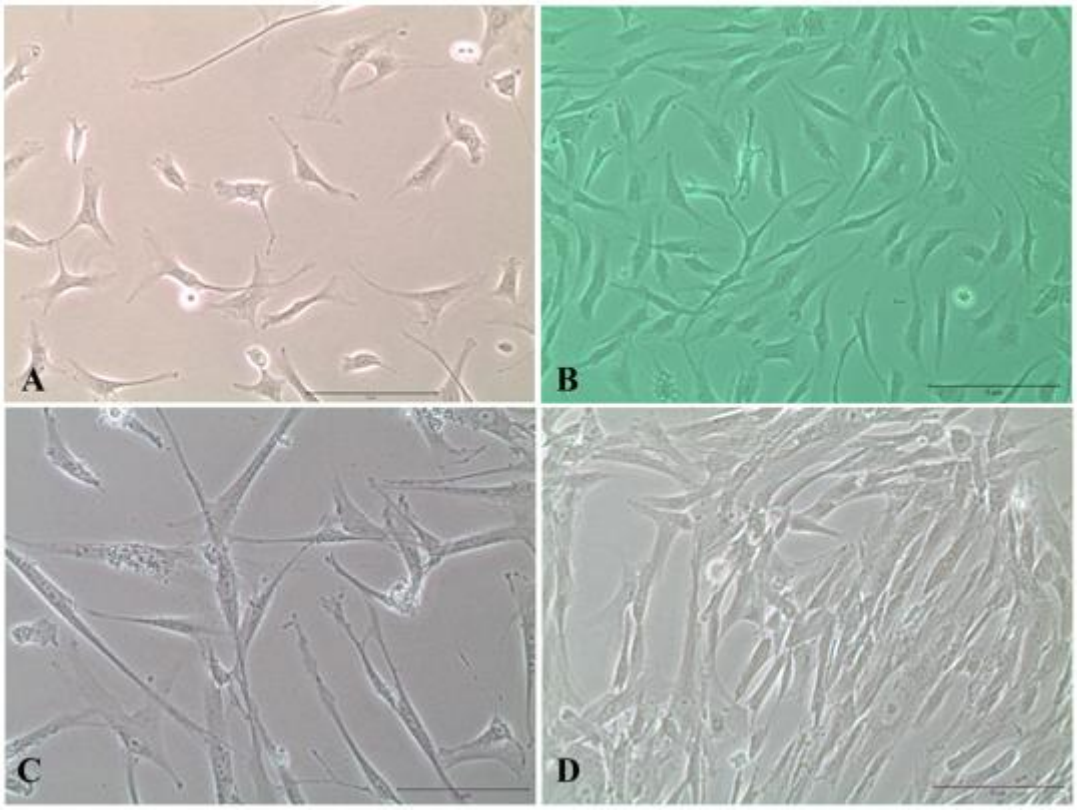

Figure 8. Micrographs of cultured mesenchymal stem cells. (a) HFPSCs early in passage (24 hours) where the cells have started to attach to the surface and proliferate. (b) Confluent HPFSC (7 days). (c) MCSCs early in passage 3 proliferating fast. (d) confluent MCSCs. MCSCs (c) in comparison to HFPSCs (a), look larger in size and have different shapes.

4.2 Cumulative population doubling level of isolated MSCs.

Isolated cells were expanded in serum-containing basal growth medium (see method). When confluent, the passaged cells were harvested and counted using trypan blue exclusion assay. For each of the passages 1 to 5, population doubling was calculated and the results are presented in table 1. To find the cumulated doubling level (cPD), the population doubling for each passage was added to the result of the previous passage. The experiment was run with two donors in both cell types. Cumulative population doubling level was used to draw a graph that illustrates the growth rate between different donors.

Table 2. Population doubling level of MCSCs and HFPSCs.

Cell type	**P-1**	**P-2**	**P-3**	**P-4**	**P-5**
MCSC –donor 1		1.08	0.56	4.45	2.06
Cumulative		1.08	1.64	6.09	8.15
MCSC – donor 2	2.14	2.16	1.5	2.95	1.74
Cumulative	2.14	4.3	5.8	8.75	10.49
Mean cumulative	**2.14**	**2.69**	**3.72**	**7.42**	**9.32**
HFPSC donor 1	0.77	1.56	5.37	1.93	1.52
Cumulative	0.77	2.33	7.70	9.63	11.15
HFPSC donor 5	1.93	0.40	1.31	2.32	1.31
Cumulative	1.93	2.33	3.64	5.96	7.27
Mean cumulative	**1.35**	**2.33**	**5.67**	**7.80**	**9.21**

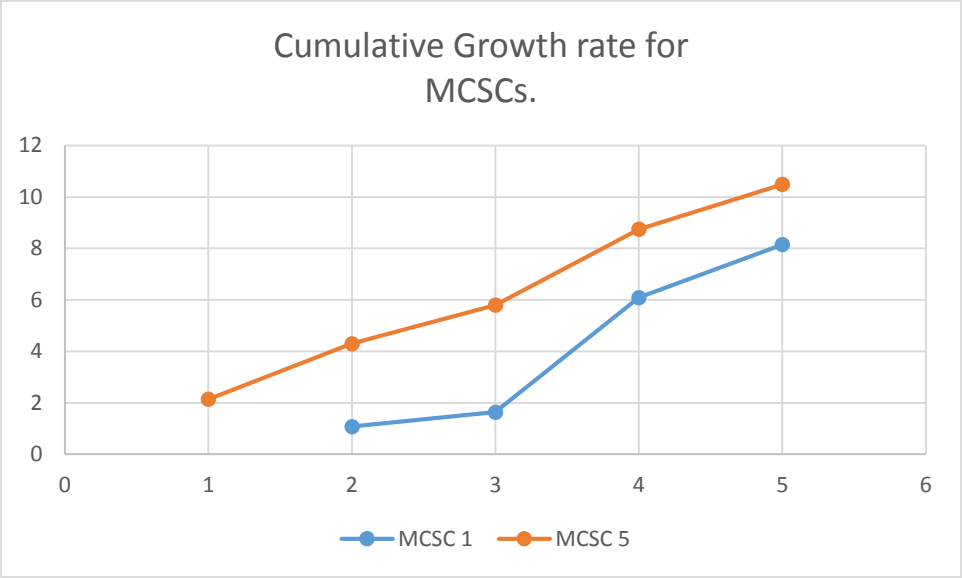

Figure 9. Comparison of the cumulative population doubling level of MCSCs from two different donors.

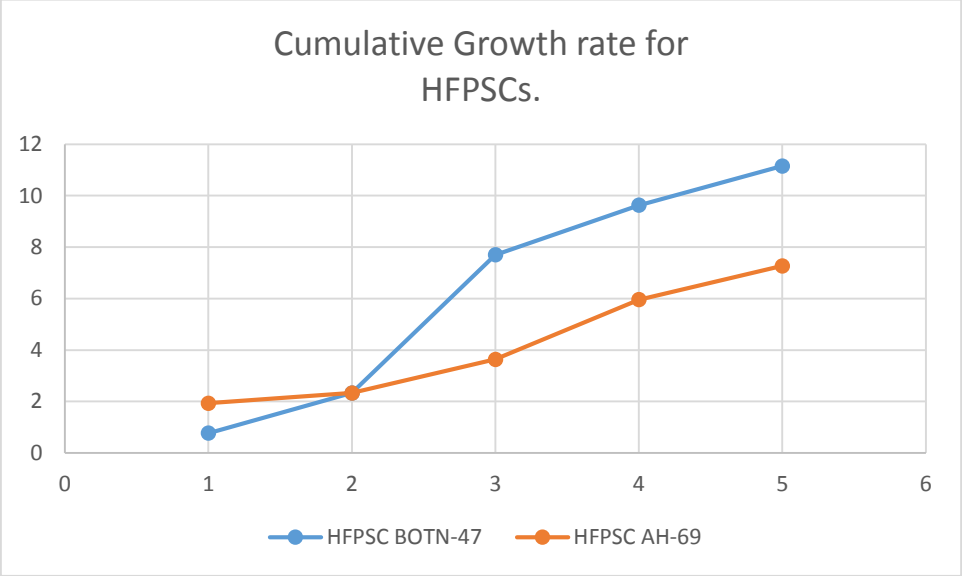

Figure 10. Comparison of the cumulative population doubling of HFPSCs from two different donors.

In addition, the mean cPD level of the two donors in each cell type was calculated and illustrated in a graph. The Graph demonstrates the growth rate of both cell types, allowing us to compare

them. The result shows that HFPSCs and MCSCs have similar growth rate, with a consistent increasing rate during the passages.

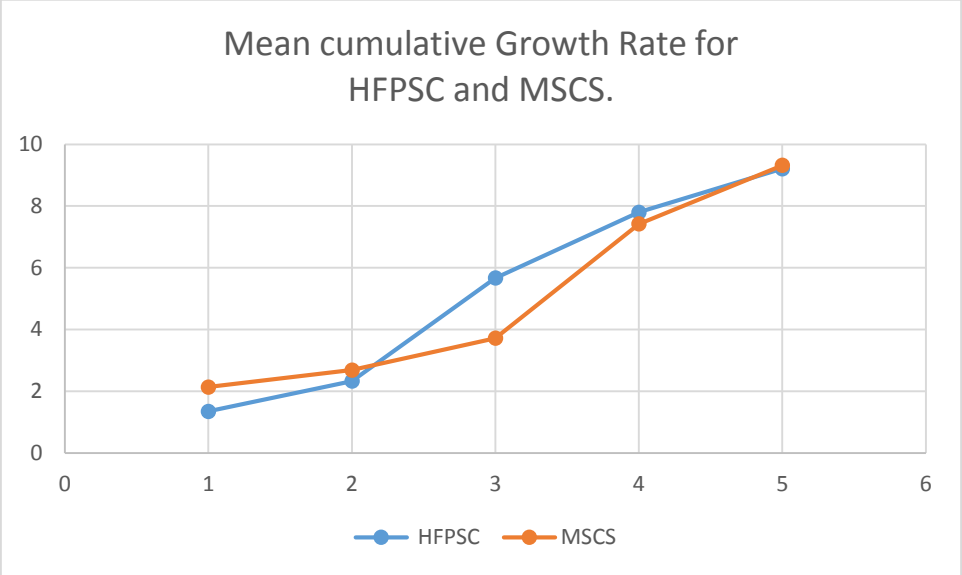

Figure 11. Mean cumulative population doubling level shows similar and constant increasing growth rate in both cells types.

4.3 Characterization of isolated cell by Flow cytometry

In order to determine the stem cell nature of isolated cells, cultures were analyzed for panel of cell surface markers by flow cytometry. The size and complexity of HFPSCs and MCSCs were analyzed and presented in dot diagrams (top panels in figure 3). Both cells types showed a positive expression of the markers CD90, CD105 and CD73, whereas cells were negative for the surface markers: CD34, CD11b, CD19, CD45 and HLA-DR. These results are in agreement with the expected phenotypic characteristics presented by mesenchymal stem cells, and confirm that the plastic-adherent, self-renewing cells in the cultures are stem-like cells. To make this assay more informative, other cell surface markers expected in some sub-sets of stem cells were also included. Both cell type showed lack of expression for CD271 and CD106, while expressing a small amount of the surface antigens CD146 and CD166. They also expressed evident amount of CD 44 antigen.

Table 3. Both of the cell types expressed phenotypic characteristics presented by mesenchymal stem cells. This analysis confirms that the isolated cells are MSCs.

Cell surface markers	**MCSC (Mixed Cord Stem Cells)**	**HFPSC (Hoffa Fat Pad Stem Cells)**
	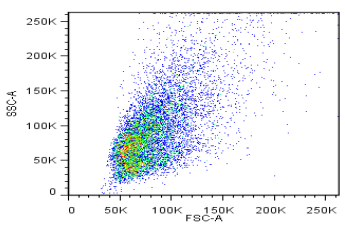	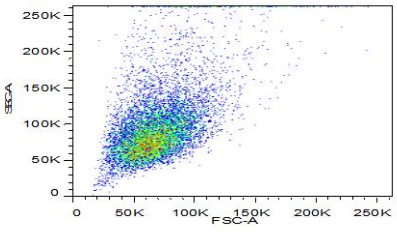
CD 90	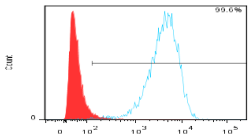	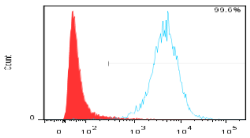
CD 105	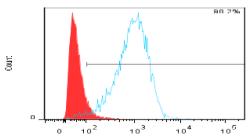	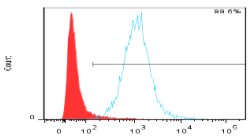
CD 73	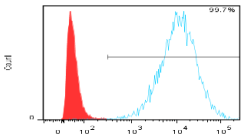	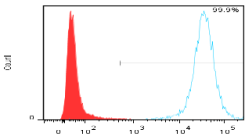
CD 34, 11b, 19, 45 & HLA-DR	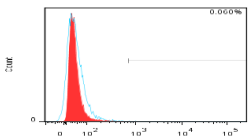	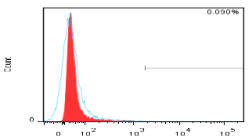
CD 44	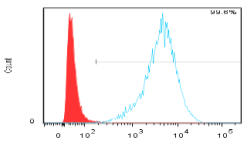	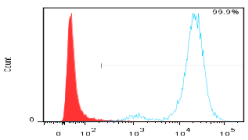

Table 3 Continued

CD 106

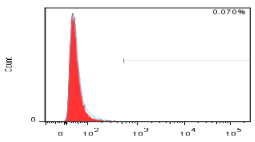

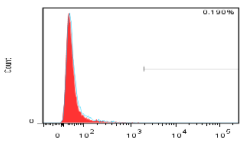

Table 4 Continued

CD 146

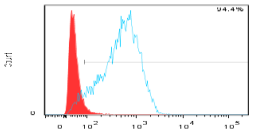

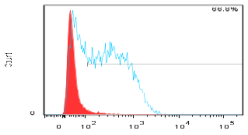

CD 166

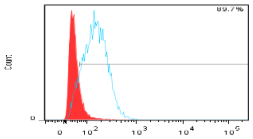

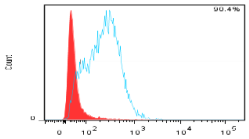

CD 271

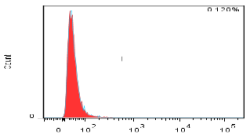

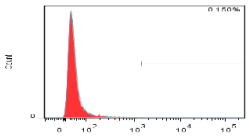

4.4 Establishment of 3-D cultures.

The isolated stem cells were expanded in monolayer and further used to construct scaffold-free 3-D cell cultures as explained in method. After three weeks in chondrogenic medium, round shaped tissue-like constructs were formed with both cell types. The pellets had a firm consistency with sharp edges. In some cases, two or more spheroids were fusing with each other making bigger tissue-like structures. This method shows that cell condensation creates cell-cell communications, development of ECM and transport of nutrients, forming more in vivo-like environment to study cell and tissue physiology. This property was seen equally in both cell types.

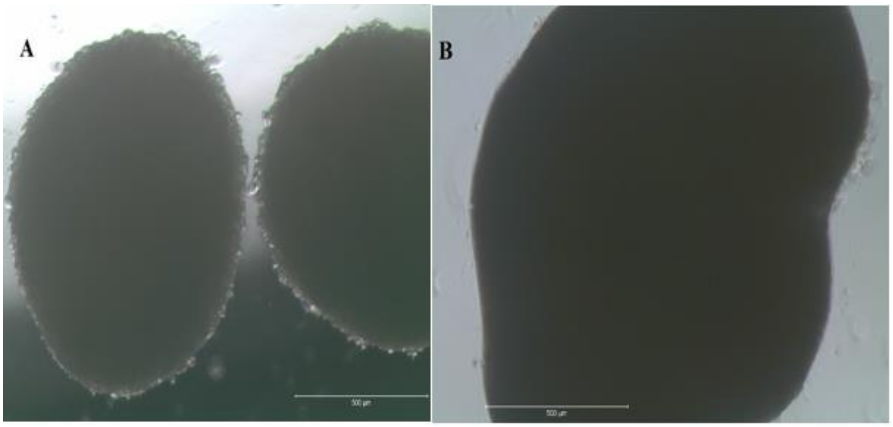

Figure 12. (a) MCSCs Spheroids on day 1. (b) On day 8, the spheroids became more firm as seen on around the spheroids. Two or more spheroids merge together to form one big tissue-like structure. Bar indicates 500 µm.

4.5 Characterization of cartilage matrix-like features in spheroids by Alcain Blue staining.

Scaffold-free 3D cell cultures were incubated for 21 days in four different combinations of chondrogenic medium. To assess the chondrogenic potential of the cells, alcian blue staining was conducted. Alcian blue solution stains sugars containing carboxyl groups, such proteoglycans and glycoproteins. Counter staining in nuclear fast red solution stains nuclei and cytoplasm, pink/red and pale pink respectively. The histological results are as presented in figure 3 and 4 where GAG was visualized with an intense dark-blue color.

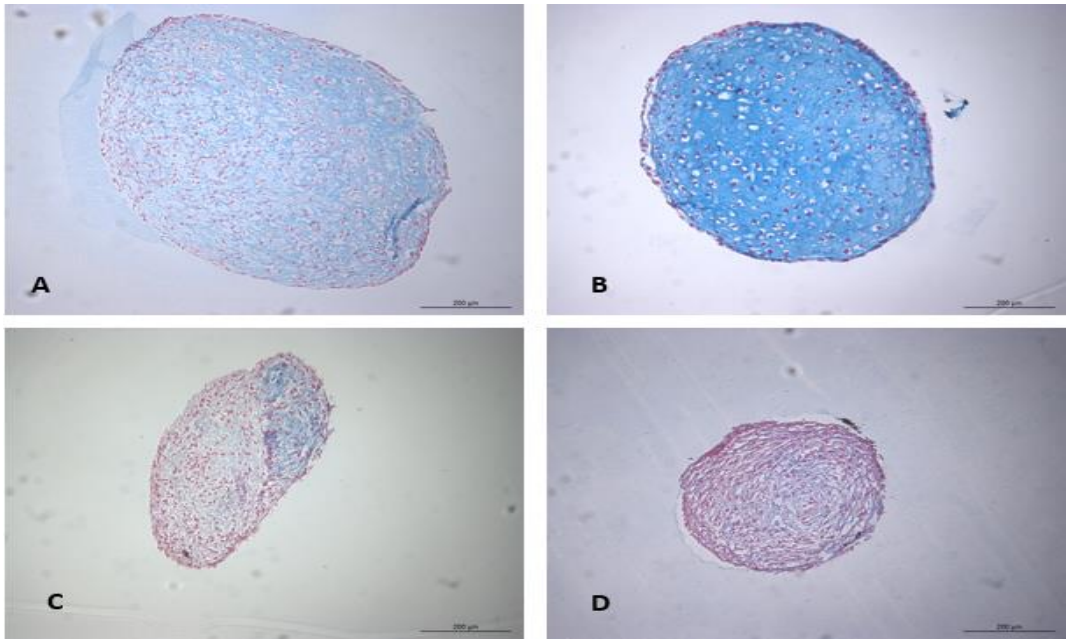

Figure 13. Light Microscopy images of HFPSCs spheroids stained with alcian blue. The spheroids were conditioned (a) in TGF-β1 + BMP-2 (b) in TGF-β3 + BMP-2 (c) in TGF-β1+ IGF-1 and (d) in TGF-β3 + IGF-1. The different chondrogenic conditions gave various results. Bar indicates 500 μm.

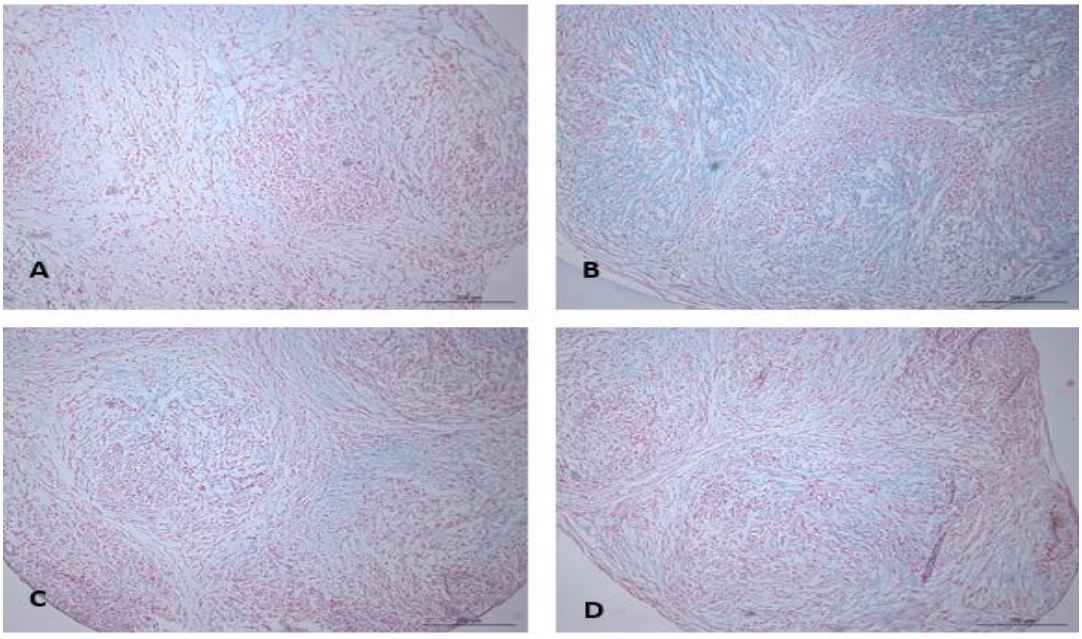

Figure 14. Light Microscopy images of mixed cord stem cell spheroids stained with alcian blue. The spheroids were conditioned (a) in TGF-β1 + BMP-2 (b) in TGF-β3 + BMP-2 (c) in TGF-β1+ IGF-1 and (d) in TGF-β3 + IGF-1. Bar indicates 500 μm.

HFPSCs kept in TGF-β3 + BMP-2 showed a successful alcian blue staining. The spheroids present abundant GAGs staining in the extracellular space as well as clearly noticeable lacunae-like structures, which is a morphological feature of hyaline cartilage. Spheroids maintained in TGF-β1 + BMP-2 show a milder blue staining with abundant chondrocyte-like cells stained in red color. The other chondrogenic medium combinations, TGF-β1+IGF-1 and TGF-β1+IGF-1, did not show proper staining of GAGs and showed low ECM content.

For the case of umbilical cord cells, alcian blue staining of MCSCs spheroids showed uniform results in all the conditions tested. All spheroids showed a very faint blue staining indicating the production of GAGs in very small amount. They contained high density of cells visualized in bright red color. When comparing the different chondrogenic media, MCSC spheroids maintained in TGF-β3 + BMP-2, showed a slightly higher blue staining than the rest, representing thus the best conditions for chondrogenesis.

When we take a closer look at the best results of both cell types, the morphological resemblance of HFPSCs with native cartilage is evident. In cartilage staining, the cells are flattened and discoid shaped in superficial zone. Further away from the articular surface, the chondrocytes become bigger with round shape. When HFPSC staining is compared with native cartilage, HFPSC have round shaped chondrocytes contained in lacuna-like structure. The GAG staining is also dark blue, similar to that of cartilage. MCSCs have numerous small cells that are not consistent in shape, and no lacunae-like structures can be recognized. MCSCs are slightly stained with alcian blue but has no morphological resemblance to cartilage.

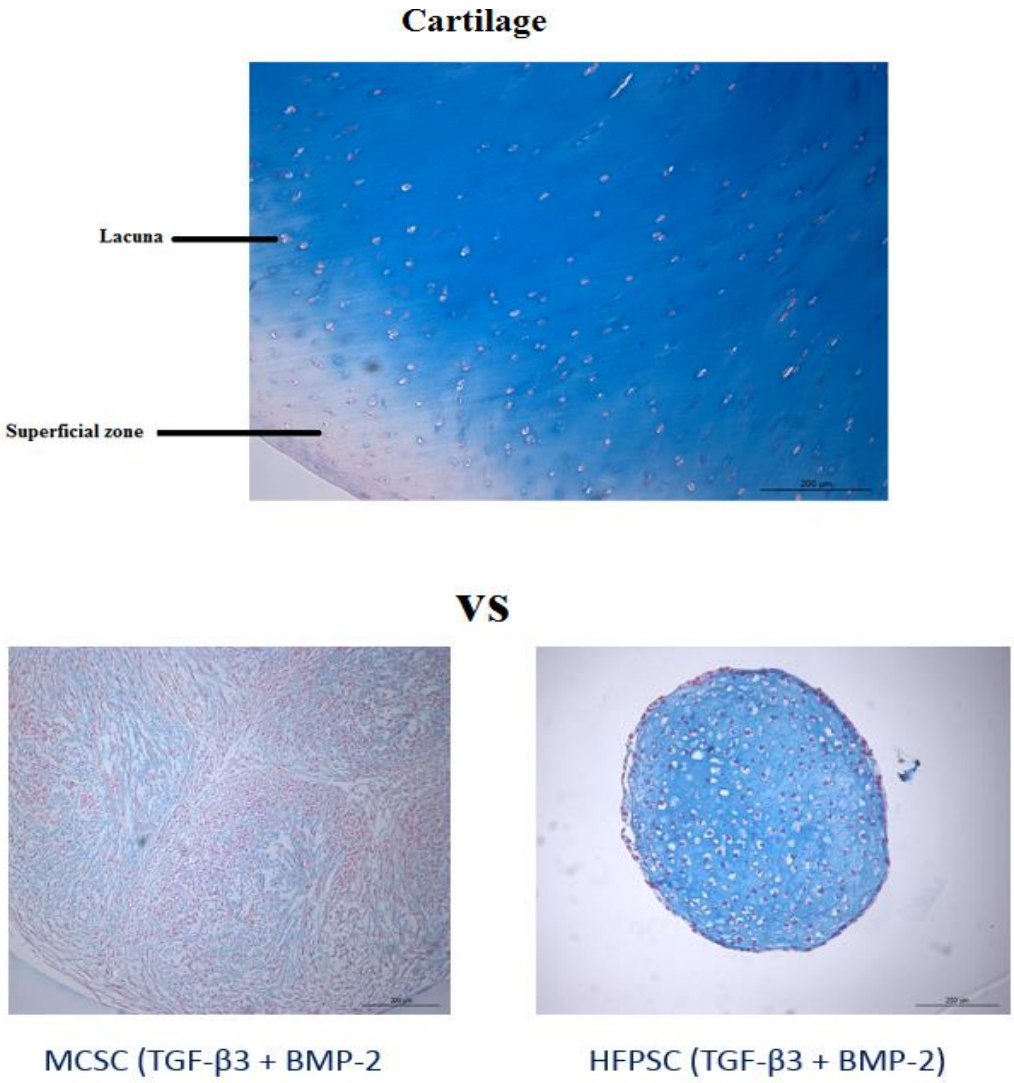

Figure 15. Comparison of light microscopy images of best condition of both cell types with alcian blue stained native cartilage. Bar indicates 500 µm.

4.6 Quantification of GAG and DNA from 3D cell culture.

HFPSC and MCSC from three different donors were used to make 3D cell spheroids. The spheroids were maintained in TGF-β3 + BMP-2 chondrogenic condition in a low oxygen level and humidified atmosphere. After 21 days, spheroids were digested by papain enzyme for GAG and DNA quantification. All test samples were run in three parallels and the average was taken for comparison (table 3).

Table 4. Concentration of DNA and GAG.

Cell type	**DNA**	**GAG**	**GAG/DNA in µg/ml**
HFPSC –donor 1	4.870	47.06	9.663
HPFSC –donor 2	1.249	13.20	10.568
HFPSC –donor 3	1.369	32.60	23.813
Mean			***14.68***
Standard deviation			***7.92***
MCSC – donor 1	1.891	29.762	15.739
MCSC – donor 5	1.136	20.825	18.332
MCSC – donor 3	2.050	25.806	12.589
Mean			***15.55***
Standard deviation			***2.88***

The mean concentration of GAG/DNA ratio was used to draw a graph. GAG/DNA ratio shows synthesis of GAG in the different cell types. Our results show that the content of GAG in spheroids from HFPSC and MCSC was rather similar when measured by this assay; however, a disturbing high variation of outcome was observed in the HFPSC group. Despite the high standard deviation, when we look at the mean GAG/DNA ratio, the difference between MCSCs and HFPSCs is very small.

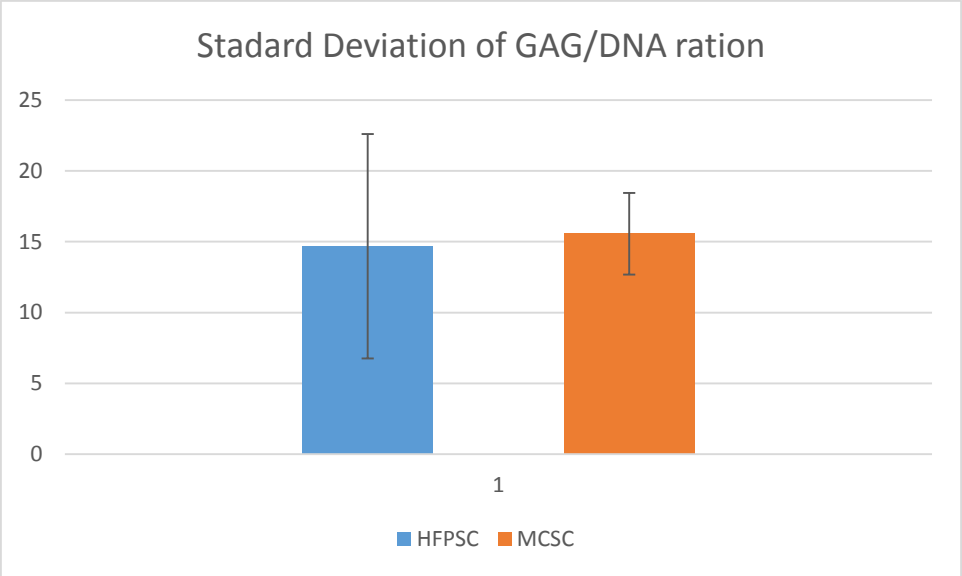

Figure 16. Average GAG/DNA ratio of MCSCs and HFPSCs. Spheroids from HFPSCs have greater standard deviation than MSCSs.

4.7 Protein identification and quantification in conditioned medium by SILAC.

Since HFPSCs showed better chondrogenenic abilities than MCSCs, the first cell type was chosen for further analyses by proteomics. After our assessment of chondrogenesis, combination of TGF-β3 + BMP-2 chondrogenic medium showed the best result on both cell types, whereas chondrogenic medium including TGF-β1 + BMP-2 was good but sub-optimal. For protein identification and quantification, we had incubated spheroids in both condition by SILAC. Unfortunately, the TGF-β3 + BMP-2 group (best chondrogenesis) contained insufficient amount of proteins required for this analysis. Due to time constraints, the experiment could not be repeated and the analyses was run with the supernatant obtained from TGF-β1 + BMP-2 group (sub-optimal medium for chondrogenesis).

HFPSCs in 2D and 3D cell culture were incubated in SILAC basal medium as explained in section 3.3.8. SILAC medium collected from 2D and 3D HFPSC cell culture was prepared by ultrafiltration and gel electrophoresis and analyzed by LC-MS spectrometry. Primary mass spectrometry (MS) values were contrasted in the Proxeon ProteinCenter software for protein identification. The carbon-13 labelled proteins found in the samples were identified and sorted according to the culture conditions. In total, 186 and 102 proteins were identified in monolayer

and in 3D spheroids medium respectively. Interestingly, 83 proteins were identified in both culture conditions. This is illustrated perfectly in a Venn diagram (figure 10).

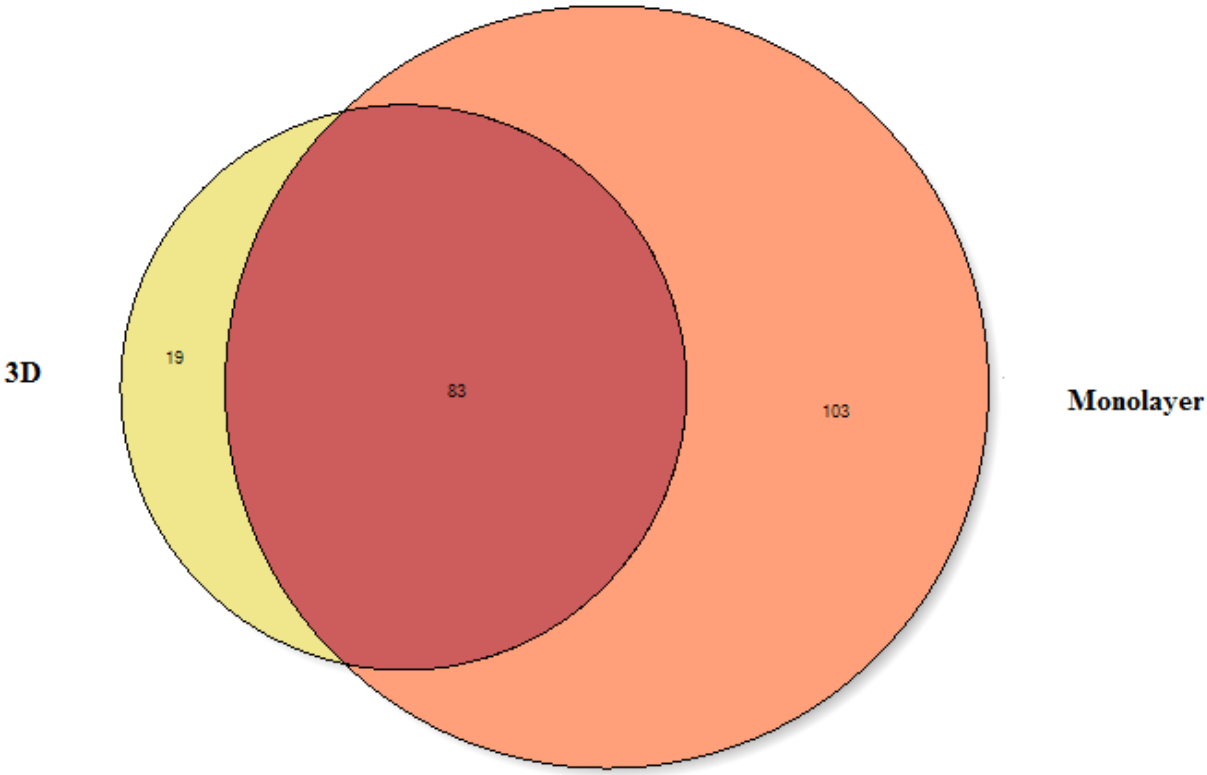

Figure 17. Carbon 13 labelled proteins identified in 3D and monolayer supernatants.

The spectra of proteins identified in supernatants of 2D and 3D HFPSCs were distributed into main clusters according to their specific functions. The percentage of each protein category from the total number of proteins identified in each experimental group is reported (table 3). The results are presented in pie charts for better illustration. The numbers on the pie chart correspond with the numbers on the table, explaining the category of identified proteins (figure 12 and 13). In both cell cultures, proteins involved in metabolic processes are the most abundant proteins. Proteins involved in cellular stress response, defense response, cell communications, or cytoskeleton associated proteins were also identified but in lower amount. In spheroids, ECM components and ECM regulatory proteins are highly expressed. This demonstrates the increased synthesis of ECM in 3D cultures.

Table 5. Identified proteins arranged according to their function.

Number	Protein Function	Protein in 2D culture		Proteins in 3D	
		Protein Amount	Percentage %	Protein Amount	Percentage %
1.	ECM components	41	12,93	24	23.76
2.	ECM regulators	27	8,52	17	16.83
3.	Metabolic processes	135	42,59	30	29.70
4.	Cytoskeleton associated proteins	16	5.05	6	5.94
5.	Defense response	12	3.79	7	6.93
6.	Cell-cell and Cell-matrix interaction	12	3.79	3	2.97
7.	Growth factors, GF inhibitors and receptors	17	5.36	4	3.96
8.	Cellular stress response	6	1.89	1	0.99
9.	Oxidative stress response	8	2.52	2	1.98
10.	Lysosomal enzyme	8	2.52	1	0.99
11.	Cell organization and biogenesis	18	5.68	2	1.98
12.	Others	17	5.36	4	3.96
	Sum	**317**		**101**	

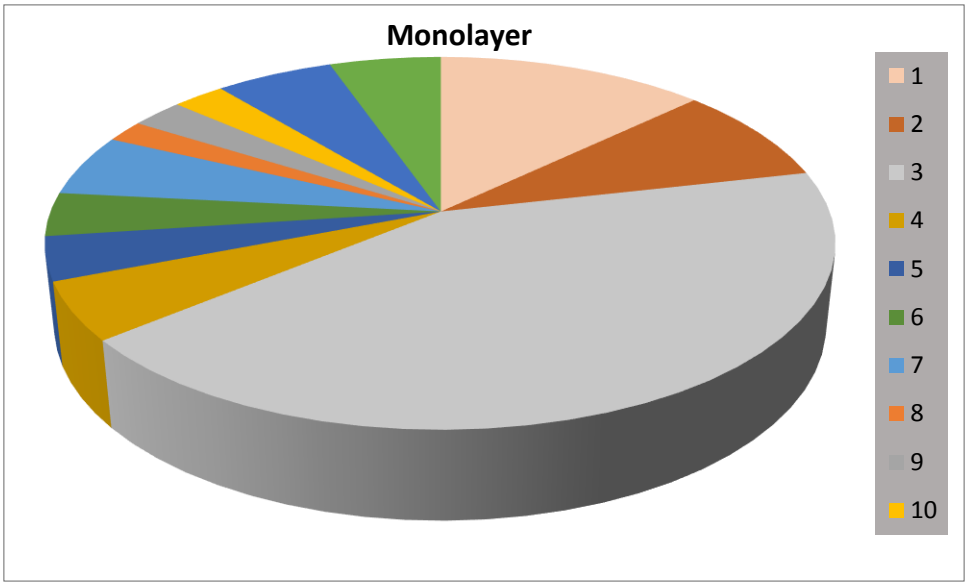

Figure 18. Proteins identified in HFPSCs monolayer cell culture. Proteins involved in metabolic processes are the most abundant, while proteins involved in cellular stress are the least expressed in 2D cell culture.

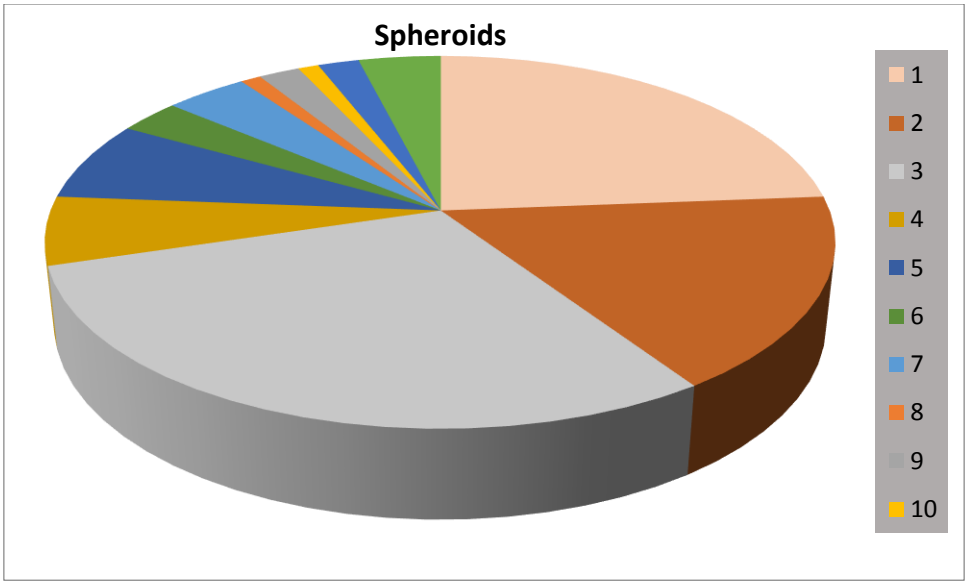

Figure 19. Pie chart illustrating proteins expressed by spheroids. Proteins involved in metabolic processes are highly expressed, while the number of lysosomal enzymes and cellular stress proteins is lower.

To gather more understanding on the phenotypic changes undergone by cells when cultured in 3D structures, proteins that were significantly up-regulated in 3D cell culture compared to 2D was calculated. Most of the significantly overexpressed molecules found in 3D conditions correspond to ECM proteins and proteins involved in regulation of ECM. Collagen type I, III, V, and XI have been identified. Most importantly, two types of collagen type II has been identified in 3D, while only one was found in 2D supernatant. These results are in line with expected outcomes from cells that are producing matrix.

Table 6. Synthesis of proteins up- regulated in 3D cell culture

Protein Name	**ACRONIM**	**PROTEINS FROM 2D**		**PROTEINS FROM 3D**		**Protein Function**
		Score	Coverage	Score	Coverage	
Cartilage oligomeric matrix protein	COMP	ND	ND	231.44	11.62	ECM
Collagen alpha-1(III) chain	COL3A1	109.06	4.02	752.74	6.62	ECM
Fibulin-2	FBLN2	94.08	2.45	141.1	6.33	ECM
TGF-beta-induced protein ig-h3	TGFBI	26.93	1.02	438.89	11.27	ECM regulation
Chitinase-3-like protein 2	CHI3L2	33.31	6.41	259.58	10	ECM
Complement factor D	CFD	104.85	6.72	148.61	6.72	Defense response
Alpha-1-antichymotrypsin	SERPINA3	ND	ND	427.86	18.91	ECM regulation

Table 6 Continued

Collagen alpha-1(I) chain	COL1A1	ND	ND	225.81	3.42	ECM
Plasma serine protease inhibitor	SERPINA5	ND	ND	130.71	10.59	ECM regulation
Collagen alpha-2(V) chain	COL5A2	ND	ND	221.91	3.37	ECM
Collagen alpha-2(I) chain	COL1A2	200.73	1.76	261.06	3	ECM
SPARC	SPARC	63.52	7.26	140.65	17.82	ECM
Collagen alpha-1(XI) chain	COL11A1	ND	ND	97.98	2.77	ECM
Collagen alpha-1(V) chain	COL5A1	ND	ND	93.06	2.33	ECM
Biglycan	BGN	ND	ND	179.28	25.27	ECM
Peptidyl-prolyl cis-trans isomerase B	PPIB	ND	ND	129.85	35.65	ECM
Fibromodulin	FMOD	50.14	10.19	40.25	5.85	ECM
Matrilysin	MMP7	ND	ND	47.16	6.37	ECM regulation

ND* - Not Identified.

One of the main aims of this study was to assess inflammatory and immune-modulatory responses of the stem cells when chondrogenically transformed in 3D culture. The spectra of proteins identified in supernatants of 2D and 3D HFPSCs were filtered according to their function and involvement in cell communication and defense response (Table 5). Classical pro-inflammatory mediators or immuno-regulators were not identified in any of the supernatants. However, components of the complement system, which are part of the innate immune system, were detected. Of importance, most of the identified growth factors and signaling molecules were found in 2D cell culture in higher amounts, whereas osteoglycin, an anabolic growth factor that acts synergistically with TGF –beta was only detected in 3D cell culture.

Table 7. Proteins involved in cell communication and defense response.

Protein Name	Acronim	PROTEINS FROM 2D		PROTEINS FROM 3D	
		Score	Coverage	Score	Coverage
Spondin 2	SPON2	91.77	4.83	38.37	2.42
Macrophage colony stimulating factor 1	CSF1	54.75	6.14	ND	ND
Growth arrest specific protein-6	GAS6	46.18	3.33	30.49	2.36
Connective tissue growth factor	CTGF	26.68	3.15	ND	ND
Trombospondin-3	TSP-3	24.12	1.67	ND	ND
Angiogenin	ANG	26.73	6.12	ND	ND
Osteoglycin	ONG	ND	ND	39.21	2.35
Complement factor D	CFD	104.85	6.72	148.61	6.72
Complement C1s	C1S	412.34	9.3	222.23	9.3
Complement C1r	C1R	155.77	8.23	380.53	21.99
Complement factor H	CFH	92.25	5.04	50.49	1.95
Galectin-1	LGALS1	47.11	11.85	ND	ND
Pentraxin-related protein PTX3	PTX3	103.81	2.36	ND	ND
Tenascin	TNC	39.47	0.37	ND	ND

ND* - Not identified.

5 Discussion

Cells with stem cell properties were isolated from Umbilical cords and Hoffa-fat pad

Mesenchymal stem cells can be obtained from various tissue types. In this study, isolation of cells from Hoffa Fat Pad (HFP) and umbilical cord (UC) was successfully achieved. To increase the number of cells isolated, after centrifugation of the digested tissue, the tissue pieces in the pellet were seed along with the cells. These primary cell are in passage zero and take long time to become confluent, usually up to 3-4 weeks. When confluent, cells were trypsinized and filtered through cell strainer before counting and reseeding for further research. Interestingly, the growth rate of the cells get higher from passage 1 and forth for as long as we passaged them. The cells becomes confluent within 7-10 days. This property was observed in both cell types.

During delivery of UC from UNN, they were kept in PBS. The cords can be kept in the refrigerator for a short period of time, but when kept for hours, isolated cells showed a very poor proliferative capacity. This could be due to cell demise and decreased number of viable cells isolated. In case of HFP, their delivery time was prescheduled and isolation of cells was always carried out right after delivery. Therefore, cell demise has not been observed in HFP tissue.

The isolated cells exhibited properties of MSCs. The cells were plastic-adherent and attached to the surface of the culture flask when seeded. As mentioned earlier, the cells had high self-renewal capacity and could be seeded in many passages without losing their proliferative ability. MCSCs showed morphological heterogeneity and variation in cell size and shape, especially during the initial stages of culture. This could be due to the various cells from the different regions of umbilical cord, since in our protocol we isolated stem cells from the whole cord (mixed cord stem cell). This morphological feature was not observed after a few passages and the cultures became more uniform.

Cumulative population doubling level was calculated to estimate the growth rate of the cells. The graph presenting MCSCs shows differences in growth rate between the different donors. However, to be able to determine whether the difference is statistically significant, T-test must be calculated. Because data independency and variation is required for T-test, we could not conduct this test. Therefore, although a difference can be seen on the graph, any conclusion

cannot be drawn. Comparison of the two cell types was done using the mean cumulative cPD level of the two donors in each cell types. As it was illustrated on the graph, both cells showed very similar growth rate with constant increasing rate up to passage 5. This demonstrates the high self-renewal capacity of stem cells.

MCSCs and HFPSCs show some differences in the expression of surface markers.

The isolated cells met one of the minimal criteria required for cells to be identified and categorized as MSCs [60]. To examine whether they possess the second property, flow cytometry was used to investigate their MSC marker phenotypes. Both HFPSCs and MCSCs expressed surface markers, CD90, CD105 and CD73, while lacking the expression of hematopoietic and other stem cells markers such as CD45. CD34, CD11b, CD19 and HLA-DR. In addition, both cells showed lack of expression for CD271 and CD106, while expressing surface markers CD146, CD166 and CD44. The differences observed between HFPSCs and MCSCs are their expression of surface antigen CD44 and CD146. It is evident that HFPSCs express more CD44 than MCSCs. The CD44 receptors (hylauronan receptors) are adhesion molecules that are expressed by many cells including chondrocytes. CD44 are abundant in pericellular matrix and are transmembrane receptors that mediate cell-cell and cell-matrix interaction, playing a great role in ECM homeostasis [106]. The stronger expression of CD44 at the cell surface of HFPSCs could be one of the factors behind the observed increased chondrogenic potential [107].

In the case of CD146, HFPSCs present two different peaks on the histogram, which indicates the existence of a sub-population of cells expressing the marker, and another sub-population of cells that express it weakly or do not express it at all. This outcome can be explained by either a transient phenotypic changes of cells during different stages of the cell cycle, or the existence of two different populations of cells with different CD146 antigen expression. In MCSCs, the expression of CD146 is more uniform, as only one peak is revealed in the histogram. Antonio Sorrentino and his colleagues have reported that human umbilical cord perivascular cells expressed higher levels of CD146 markers compared to BMSCs [108]. CD146, also known as melanoma cell adhesion molecule, is primarily expressed by vascular endothelium and smooth muscle cells in normal adult tissue. In some studies, a strong expression of this molecule has

been associated with commitment to a vascular smooth muscle cell lineage [109]. On the other hand, a latest study have demonstrated that chondroprogenitor cells expressing high level of CD146 show higher chondrogenic capacity [109], something which is not observed by us. Therefore, any speculation regarding CD146 and chondrogenic ability of the MCSCs is difficult.

HFPSCs show superior chondrogenic capacity than MCSCs

Chondrogenically induced spheroids were stained with Alcian blue solution to visualize glycosaminoglycans. Spheroids constructed from HFPSCs and cultured in TGF-β3 + BMP-2, presented the best result so far. The pellets stained intense blue color showing equally distributed GAG throughout the tissue. Unlike HFPSCs, 3D cultures of MCSCs did not stain with alcian blue very much. The tissue contained high density of cells, some ECM but showed low GAGs content. Although not significantly, the spheroids incubated in TGF-β3 + BMP-2 showed most staining compared with the rest of the chondrogenic medium combination.

Transforming growth factor beta (TGF- β) is a superfamily that consists of a large group of molecules including TGF- β isoforms and bone morphogenetic proteins (BMPs), and has an important role in cell proliferation and differentiation. Bone morphologic proteins are cytokines that induce bone and cartilage formation and signal through transmembrane serine/threonine kinase receptors. The receptors are composed of type I and II subtypes and Smad protein family that are part of type I receptor. BMPs bind to both types of receptors and form ligand-receptor complex resulting in phosphorylation of Smad that leads signal to the nucleus for gene transcription [110]. BMP-2 added to a 3D cell culture has shown to enhance the expression of collagen type II, which is one of the characteristic components of cartilage [111]. Application of 100 ng/ml BMP-2 has proven to increase the synthesis of proteoglycan near maximal [112].

TGF-β play an important role in cell proliferation, condensation and chondrogenesis. Addition of TGF-β3 in the medium in pellets of aggregated cells induces chondrogenesis and have been extensively used in cellular studies [51, 113, 114]. There are three types of TGF-β receptors by which they elicit their signal, type I, type II and type III. Ligand binding type II receptor activates type I receptor, which in turn phosphorylates Smad protein family [115]. The third receptor (betaglycan) can modulate response by both extracellular and cytoplasmic domains,

enhancing cell responsiveness [116]. Betaglycans are widely distributed in some cells including mesenchymal stem cells. When BMP-2 + TGF-β3 are used in combination, the effect of TGF-β3 is significantly enhanced, augmenting ECM production [117]. This effect is evident in our study, confirming the findings of previous case reports. The spheroids maintained in TGF-β3 + BMP-2 stained intensely with alcian blue, detecting the presence of GAG in high amount. Their morphology resembles that of native cartilage, with chondrocytes stained pink and surrounded by lacuna-like structure.

TGF- β1 has shown to initiate chondrogenesis in 3D cultures incubated serum-free medium [118]. The up-regulation of superficial zone protein, lubiricin, that has an important function in lubrication of the joint has been documented[119]. In our study, HFPSCs spheroids incubated in TGF-β1 + BMP-2 showed a milder staining than after incubation with TGF-β3 + BMP-2.

Even though it has been reported that MSCs express insulin-like growth factor-1 (IGF-I), there are contradictory results regarding their chondrogenic effect. Most studies have reported that IGF-I has no effect on MSCs or has effect only in combination with TGF-β. A study conducted in the absence or/and presence of IGF-I and TGF-β1 has shown that IGF-I had equally potent chondrogenic effect as TGF-β1. Their effect was independent and additive [120]. In contrast, the chondrogenic mediums consisting IGF-1 did not produce good results in either HFPSCs or MCSCs in our study.

DNA and GAG quantification assay conducted revealed somehow contradictory result, since about equal levels of GAGs where measured in spheroids from HFPSCs and MCSCs. It should be noted that GAGs levels from the three HFPSC donors had a high intra-group variability. This biochemical assay is still under development in our laboratory and we suspect that some inconsistencies could be generated if papain digestion of spheroids is not even. For this reason we are more confident on results showing alcian blue staining, which additionally, permits assess other aspects of tissue characteristics relevant in the context of cartilage such as the round shape of cells, the formation of lacunae-like structure or the increase extracellular matrix deposition. Therefore, we conclude that HFPSCs have higher chondrogenesis potential than MCSCs.

Increased matrix synthesis after chondrogenic differentiation in 3D spheroids is revealed by analyzing the secretome.

One of the purpose of this project was to investigate the changes in the cell phenotypes before and after differentiation by secretomics. Since HFPSCs presented the most prominent cartilage differentiation abilities, we conducted comparative protein expression analysis on conditioned medium from 2D (monolayer) and 3D (spheroids) cell cultures using SILAC technology. In total, 186 and 102 proteins were identified in monolayer and in 3D cell culture medium respectively. Although more proteins are identified in supernatants from monolayer cell culture, it does not necessary mean that cells in this condition have higher protein synthesis. Cells cultured in monolayer are more exposed to the medium, which may results in more protein concentration in the medium. Another reasonable explanation can be the assembling and entrapment of released proteins in extracellular matrix in 3D cell structures. The spectra of proteins identified in supernatants of 2D and 3D HFPSCs were distributed into main clusters according to their specific functions. The most abundant proteins in both cell cultures systems are proteins involved in metabolic processes. A clear difference is that HFPSCs in 3D culture show higher number of ECM components and regulators than in 2D cultures. Of importance, in quantitative analysis most of the significantly over expressed proteins found in 3D conditions correspond to ECM structural components, confirming that high cell density promotes extracellular matrix depositions and chondrogenesis. It is also proves that HFPSCs indeed have high chondrogenic potential. Expression of COMP, a noncollagenous ECM protein that binds fibrils playing an important role in cartilage maintenance and strength, was enhanced in 3D supernatant while absent in monolayer. All types of collagens were significantly over expressed in 3D, while most were absent in 2D supernatants. Collagen type II, which is one of the characteristic components of cartilage, was identified in 3D supernatant. When collagen type II is synthesized, it immediately gets incorporated in the newly formed ECM. The soluble collagen type II that is identified in supernatant shows that 3D culture has high expression. Another important ECM component absent in 2D but identified in 3D is, matrix metalloproteinases-7 (MMP7), a protease responsible for degradation of ECM that targets collagen type I and aggrecan. These results demonstrate a process of extracellular matrix development and turnover present in 3D. Similar to our finding, a secretomic study on human MSCs undergoing chondrogenic differentiation demonstrated that most of the identified proteins were characteristic of cartilage ECM [121].

Chondrogenic differentiation do not promote changes in the release of inflammatory or immunomodulatory molecules.

In assessment of their inflammatory and immunogenic responses, the classical pro-inflammatory mediators or immune regulators were not detected in either the 2D or 3D cell culture supernatants. However, presence of components of the complement system was shown. Most of the components, such as complement C1s, complement C1r and complement factor D, are over expressed in 3D supernatant. Pentraxin-related protein (PTX3) is produced in response to primary inflammatory signals and was detected in 2D culture supernatants. Macrophage colony stimulating factor 1 is another cytokine that is only identified in 2D culture medium. Chen et al., reported that chondrogenic differentiation of MSCs increase their immunogenicity leading to stimulation of DCs [122]. Ryan et al., also showed that chondrogenically differentiated MSCs are not fully immunoprivileged and induced T-cell responses [123]. A recent study has reported a contradictory result. An *in vitro* study on adipose derived stem cells has demonstrated up-regulation of INF-γ, interleukin (IL)-10 in TGF-β3-induced chondrogensis [124]. Proteomics permits the identification of a broad spectrum of proteins from a given biological sample, however it may lack the sensitivity that other techniques provide. We think therefore that our study should be complemented by analyzing supernatants with more sensitive antibody-based detection approaches.

Osteoglycin (mimecan) was the only component that was not identified in 2D cell culture (table 5). The secretion of components of the innate immune response and osteoglycin was reported in chondrocytes when their toll-like receptors are activated. Similar to our findings, the investigators did not detect TNF-α nor IL-1 [125]. The activation of TLR that leads to production of osteoglycin in articular chondrocytes has been associated with the catabolism and degradation of matrix. In addition, osteoglycin is a proteoglycan that induces ectopic bone formation and its expression by chondrocytes is undesired. This process occurs by osteoglycin in conjunction with TGF- β [126]. Aki Osawa and his colleague conducted a study on activation of genes for growth factor and cytokines involved in chondrogenic differentiation. They reported high expression of osteoglycin in the late phase of chondrocyte differentiation and in

hypertrophic chondrocytes. Osteoglycin bind BMP-2 and releases it in the ECM. Based on this information, the presence of osteoglycin in 3D cell culture indicates that the HFPSCs have successfully differentiated into chondrocytes [127].

6 Conclusion

1) Isolation of mesenchymal stem cells from specimens of Hoffa-fat pad and umbilical cord was achieved in a relatively simple and reproducible way. The isolated cells were adherent to the surface of culture flask and had similar proliferative capacity.

2) Examination of the cell phenotypes by flow cytometry showed positive expression of surface markers: CD90, CD105 and CD73, while lacking the expression of hematopoietic and other stem cells markers such as CD45. CD34, CD11b, CD19 and HLA-DR, fulfilling the minimal requirement for mesenchymal stem cells surface antigen expression.

3) Upon chondrogenic induction in cell pellets, HFPSCs showed superior chondrogenic capacity than MCSCs.

4) Histological and biochemical assessment of the 3D constructs showed that cell pellets maintained in combination of TGF-β3 + BMP-2 were the best option for synthesis of GAGs and morphological resemblance with native cartilage.

5) Comparison of protein expression analysis on conditioned medium from 2D (monolayer) and 3D (spheroids) cell cultures using SILAC technology revealed that spheroids had high expression of ECM components and regulators than monolayer.

6) Classical pro-inflammatory mediators or immune regulators were not detected in supernatants of 2D and 3D cultures indicating that chondrogenic differentiation do not activate inflammatory or immune reactions.

7 Future aspects

The establishment of scaffold-free 3-D cell culture has been successful. Hoffa-fat pad derived stem cells presented a great chondrogenic potential when maintained in TGF-β3 + BMP-2. Some of our analyses are incomplete. In the future;

1) Other assays such as gene expression and immunohistochemistry can be used to assess chondrogenic differentiation potential of the cells. Immunohistochemistry with anti-Collagen I and II antibodies can provide the structure and integrity of the extracellular matrix synthesized by the spheroids.

2) For better investigation of the inflammatory and immunogenic responses of the differentiated cells, a more sensitive technique that can identify proteins released in a very low amount should be used.

3) Hoffa-fat pad-derived stem cells can be used to make scaffold-based 3D cultures than can be used in *in vivo* studies to provide more relevant information for clinical use of the cells in cartilage repair.

References

1. Helmick, C.G., et al., *Estimates of the prevalence of arthritis and other rheumatic conditions in the United States. Part I.* Arthritis Rheum, 2008. **58**(1): p. 15-25.
2. Kvien, T.K., et al., *The prevalence and severity of rheumatoid arthritis in Oslo. Results from a county register and a population survey.* Scand J Rheumatol, 1997. **26**(6): p. 412-8.
3. Pacifici, M., E. Koyama, and M. Iwamoto, *Mechanisms of synovial joint and articular cartilage formation: recent advances, but many lingering mysteries.* Birth Defects Research Part C: Embryo Today: Reviews, 2005. **75**(3): p. 237-248.
4. McDevitt, C.A., *Biochemistry of articular cartilage. Nature of proteoglycans and collagen of articular cartilage and their role in ageing and in osteoarthrosis.* Annals of the Rheumatic Diseases, 1973. **32**(4): p. 364-378.
5. Kuettner, K.E., *Biochemistry of articular cartilage in health and disease.* Clinical biochemistry, 1992. **25**(3): p. 155-163.
6. <*The chondrocyte.pdf*>.
7. Eggli, P.S., E.B. Hunziker, and R.K. Schenk, *Quantitation of structural features characterizing weight- and less-weight-bearing regions in articular cartilage: a stereological analysis of medial femoral condyles in young adult rabbits.* Anat Rec, 1988. **222**(3): p. 217-27.
8. Kheir, E. and D. Shaw, *Hyaline articular cartilage.* Orthopaedics and Trauma, 2009. **23**(6): p. 450-455.
9. Poole, C.A., M.H. Flint, and B.W. Beaumont, *Chondrons in cartilage: ultrastructural analysis of the pericellular microenvironment in adult human articular cartilages.* Journal of orthopaedic research, 1987. **5**(4): p. 509-522.
10. Huber, M., S. Trattnig, and F. Lintner, *Anatomy, biochemistry, and physiology of articular cartilage.* Investigative radiology, 2000. **35**(10): p. 573-580.
11. Poole, C.A., M. Flint, and B. Beaumont, *Morphological and functional interrelationships of articular cartilage matrices.* Journal of anatomy, 1984. **138**(Pt 1): p. 113.
12. Hoemann, C.D., *Molecular and biochemical assays of cartilage components*, in *Cartilage and osteoarthritis*. 2004, Springer. p. 127-156.
13. Poole, C.A., A. Matsuoka, and J.R. Schofield, *Chondrons from articular cartilage: III. Morphologic changes in the cellular microenvironment of chondrons isolated from osteoarthritic cartilage.* Arthritis and Rheumatism, 1991. **34**(1): p. 22-35.
14. Mollenhauer, J., et al., *Role of anchorin CII, a 31,000-mol-wt membrane protein, in the interaction of chondrocytes with type II collagen.* The Journal of cell biology, 1984. **98**(4): p. 1572-1579.
15. Durr, J., et al., *Localization of beta 1-integrins in human cartilage and their role in chondrocyte adhesion to collagen and fibronectin.* Exp Cell Res, 1993. **207**(2): p. 235-44.
16. Mayne, R., *Cartilage collagens. What is their function, and are they involved in articular disease?* Arthritis & Rheumatism, 1989. **32**(3): p. 241-246.
17. Hollander, A.P., et al., *Damage to type II collagen in aging and osteoarthritis starts at the articular surface, originates around chondrocytes, and extends into the cartilage with progressive degeneration.* J. Clin. Invest., 1995. **96**(6): p. 2859-2869.
18. Kempson, G.E., et al., *The tensile properties of the cartilage of human femoral condyles related to the content of collagen and glycosaminoglycans.* Biochim Biophys Acta, 1973. **297**(2): p. 456-72.
19. Vaughan, L., et al., *D-periodic distribution of collagen type IX along cartilage fibrils.* The Journal of cell biology, 1988. **106**(3): p. 991-997.
20. Muller-Glauser, W., et al., *On the role of type IX collagen in the extracellular matrix of cartilage: type IX collagen is localized to intersections of collagen fibrils.* J Cell Biol, 1986. **102**(5): p. 1931-9.

21. Bruckner, P., L. Vaughan, and K.H. Winterhalter, *Type IX collagen from sternal cartilage of chicken embryo contains covalently bound glycosaminoglycans.* Proc Natl Acad Sci U S A, 1985. **82**(9): p. 2608-12.
22. Mendler, M., et al., *Cartilage contains mixed fibrils of collagen types II, IX, and XI.* J Cell Biol, 1989. **108**(1): p. 191-7.
23. Wu, J.J. and D.R. Eyre, *Structural analysis of cross-linking domains in cartilage type XI collagen. Insights on polymeric assembly.* J Biol Chem, 1995. **270**(32): p. 18865-70.
24. Hardingham, T.E. and H. Muir, *Hyaluronic acid in cartilage and proteoglycan aggregation.* Biochem. J, 1974. **139**: p. 565-581.
25. Poole, A., et al., *An immunoelectron microscope study of the organization of proteoglycan monomer, link protein, and collagen in the matrix of articular cartilage.* The Journal of cell biology, 1982. **93**(3): p. 921-937.
26. Mow, V.C., et al., *The influence of link protein stabilization on the viscometric properties of proteoglycan aggregate solutions.* BBA - General Subjects, 1989. **992**(2): p. 201-208.
27. Kempson, H., et al., *Correlations between stiffness and the chemical constituents of cartilage on the human femoral head.* BBA - General Subjects, 1970. **215**(1): p. 70-77.
28. Hollander, A.P., et al., *Increased damage to type II collagen in osteoarthritic articular cartilage detected by a new immunoassay.* Journal of Clinical Investigation, 1994. **93**(4): p. 1722.
29. Venn, M. and A. Maroudas, *Chemical composition and swelling of normal and osteoarthrotic femoral head cartilage. I. Chemical composition.* Ann Rheum Dis, 1977. **36**(2): p. 121-9.
30. Van Den Borne, M., et al., *International Cartilage Repair Society (ICRS) and Oswestry macroscopic cartilage evaluation scores validated for use in Autologous Chondrocyte Implantation (ACI) and microfracture.* Osteoarthritis and Cartilage, 2007. **15**(12): p. 1397-1402.
31. Deng, C., et al., *Fibroblast growth factor receptor 3 is a negative regulator of bone growth.* Cell, 1996. **84**(6): p. 911-921.
32. Hunter, A.G., J.T. Hecht, and C.I. Scott, Jr., *Standard weight for height curves in achondroplasia.* Am J Med Genet, 1996. **62**(3): p. 255-61.
33. Trentham, D.E. and C.H. Le, *Relapsing polychondritis.* Annals of Internal Medicine, 1998. **129**(2): p. 114-122.
34. Hubertsson, J., et al., *Sick leave patterns in common musculoskeletal disorders--a study of doctor prescribed sick leave.* BMC Musculoskelet Disord, 2014. **15**: p. 176.
35. Dahaghin, S., et al., *Prevalence and pattern of radiographic hand osteoarthritis and association with pain and disability (the Rotterdam study).* Annals of the rheumatic diseases, 2005. **64**(5): p. 682-687.
36. Merx, H., et al., *International variation in hip replacement rates.* Annals of the rheumatic diseases, 2003. **62**(3): p. 222-226.
37. Benito, M.J., et al., *Synovial tissue inflammation in early and late osteoarthritis.* Annals of the rheumatic diseases, 2005. **64**(9): p. 1263-1267.
38. Lee, K.M., et al., *Risk factors for osteoarthritis and contributing factors to current arthritic pain in South korean older adults.* Yonsei Med J, 2015. **56**(1): p. 124-31.
39. Felson, D.T., et al., *The prevalence of knee osteoarthritis in the elderly. The Framingham Osteoarthritis Study.* Arthritis & Rheumatism, 1987. **30**(8): p. 914-918.
40. Kempson, G.E., *Age-related changes in the tensile properties of human articular cartilage: a comparative study between the femoral head of the hip joint and the talus of the ankle joint.* Biochim Biophys Acta, 1991. **1075**(3): p. 223-30.
41. Stecher, R.M. and A. Hersh, *Heberden's nodes: the mechanism of inheritance in hypertrophic arthritis of the fingers.* Journal of Clinical Investigation, 1944. **23**(5): p. 699.
42. Spector, T.D. and A.J. MacGregor, *Risk factors for osteoarthritis: genetics.* Osteoarthritis Cartilage, 2004. **12 Suppl A**: p. S39-44.

43. Davis, M.A., W.H. Ettinger, and J.M. Neuhaus. *Obesity and osteoarthritis of the knee: evidence from the National Health and Nutrition Examination Survey (NHANES I)*. in *Seminars in arthritis and rheumatism*. 1990. Elsevier.
44. Loeuille, D., et al., *Macroscopic and microscopic features of synovial membrane inflammation in the osteoarthritic knee: correlating magnetic resonance imaging findings with disease severity.* Arthritis Rheum, 2005. **52**(11): p. 3492-501.
45. Bobinac, D., et al., *Changes in articular cartilage and subchondral bone histomorphometry in osteoarthritic knee joints in humans.* Bone, 2003. **32**(3): p. 284-290.
46. Aurich, M., et al., *Differential matrix degradation and turnover in early cartilage lesions of human knee and ankle joints.* Arthritis & Rheumatism, 2005. **52**(1): p. 112-119.
47. Stefan Lohmander, L., P.J. Neame, and J.D. Sandy, *The structure of aggrecan fragments in human synovial fluid. Evidence that aggrecanase mediates cartilage degradation in inflammatory joint disease, joint injury, and osteoarthritis.* Arthritis & Rheumatism, 1993. **36**(9): p. 1214-1222.
48. Bondeson, J., et al., *The role of synovial macrophages and macrophage-produced cytokines in driving aggrecanases, matrix metalloproteinases, and other destructive and inflammatory responses in osteoarthritis.* Arthritis research & therapy, 2006. **8**(6): p. R187.
49. Sandy, J.D., et al., *The structure of aggrecan fragments in human synovial fluid. Evidence for the involvement in osteoarthritis of a novel proteinase which cleaves the Glu 373-Ala 374 bond of the interglobular domain.* Journal of Clinical Investigation, 1992. **89**(5): p. 1512.
50. Thomson, J.A., et al., *Embryonic stem cell lines derived from human blastocysts.* Science, 1998. **282**(5391): p. 1145-7.
51. Pittenger, M.F., et al., *Multilineage potential of adult human mesenchymal stem cells.* Science, 1999. **284**(5411): p. 143-7.
52. Halleux, C., et al., *Multi-lineage potential of human mesenchymal stem cells following clonal expansion.* J Musculoskelet Neuronal Interact, 2001. **2**(1): p. 71-6.
53. Tropel, P., et al., *Isolation and characterisation of mesenchymal stem cells from adult mouse bone marrow.* Exp Cell Res, 2004. **295**(2): p. 395-406.
54. Oswald, J., et al., *Mesenchymal stem cells can be differentiated into endothelial cells in vitro.* Stem cells, 2004. **22**(3): p. 377-384.
55. Yamazaki, H., et al., *Potential of dental mesenchymal cells in developing teeth.* Stem Cells, 2007. **25**(1): p. 78-87.
56. Miao, Z., et al., *Isolation of mesenchymal stem cells from human placenta: comparison with human bone marrow mesenchymal stem cells.* Cell Biol Int, 2006. **30**(9): p. 681-7.
57. Kern, S., et al., *Comparative analysis of mesenchymal stem cells from bone marrow, umbilical cord blood, or adipose tissue.* Stem cells, 2006. **24**(5): p. 1294-1301.
58. Lu, L.-L., et al., *Isolation and characterization of human umbilical cord mesenchymal stem cells with hematopoiesis-supportive function and other potentials.* haematologica, 2006. **91**(8): p. 1017-1026.
59. Horwitz, E.M., et al., *Clarification of the nomenclature for MSC: The International Society for Cellular Therapy position statement.* Cytotherapy, 2005. **7**(5): p. 393-5.
60. Dominici, M., et al., *Minimal criteria for defining multipotent mesenchymal stromal cells. The International Society for Cellular Therapy position statement.* Cytotherapy, 2006. **8**(4): p. 315-7.
61. Zuk, P.A., et al., *Human adipose tissue is a source of multipotent stem cells.* Mol Biol Cell, 2002. **13**(12): p. 4279-95.
62. Guilak, F., et al., *Clonal analysis of the differentiation potential of human adipose-derived adult stem cells.* Journal of cellular physiology, 2006. **206**(1): p. 229-237.
63. Wickham, M.Q., et al., *Multipotent stromal cells derived from the infrapatellar fat pad of the knee.* Clinical orthopaedics and related research, 2003. **412**: p. 196-212.
64. Peng, L., et al., *Comparative analysis of mesenchymal stem cells from bone marrow, cartilage, and adipose tissue.* Stem cells and development, 2008. **17**(4): p. 761-774.

65. Li, H., et al., *Adipogenic potential of adipose stem cell subpopulations.* Plast Reconstr Surg, 2011. **128**(3): p. 663-72.
66. McIntosh, K., et al., *The Immunogenicity of Human Adipose-Derived Cells: Temporal Changes In Vitro.* Stem cells, 2006. **24**(5): p. 1246-1253.
67. Puissant, B., et al., *Immunomodulatory effect of human adipose tissue-derived adult stem cells: comparison with bone marrow mesenchymal stem cells.* British journal of haematology, 2005. **129**(1): p. 118-129.
68. Zuk, P.A., et al., *Human adipose tissue is a source of multipotent stem cells.* Molecular biology of the cell, 2002. **13**(12): p. 4279-4295.
69. Mennan, C., et al., *Isolation and characterisation of mesenchymal stem cells from different regions of the human umbilical cord.* Biomed Res Int, 2013. **2013**: p. 916136.
70. Kadivar, M., et al., *In vitro cardiomyogenic potential of human umbilical vein-derived mesenchymal stem cells.* Biochemical and biophysical research communications, 2006. **340**(2): p. 639-647.
71. Wang, H.S., et al., *Mesenchymal stem cells in the Wharton's jelly of the human umbilical cord.* Stem cells, 2004. **22**(7): p. 1330-1337.
72. Deuse, T., et al., *Immunogenicity and immunomodulatory properties of umbilical cord lining mesenchymal stem cells.* Cell Transplant, 2011. **20**(5): p. 655-67.
73. Sarugaser, R., et al., *Human umbilical cord perivascular (HUCPV) cells: a source of mesenchymal progenitors.* Stem cells, 2005. **23**(2): p. 220-229.
74. Romanov, Y.A., V.A. Svintsitskaya, and V.N. Smirnov, *Searching for alternative sources of postnatal human mesenchymal stem cells: candidate MSC-like cells from umbilical cord.* Stem cells, 2003. **21**(1): p. 105-110.
75. Le Blanc, K., et al., *Mesenchymal stem cells inhibit and stimulate mixed lymphocyte cultures and mitogenic responses independently of the major histocompatibility complex.* Scandinavian journal of immunology, 2003. **57**(1): p. 11-20.
76. Di Nicola, M., et al., *Human bone marrow stromal cells suppress T-lymphocyte proliferation induced by cellular or nonspecific mitogenic stimuli.* Blood, 2002. **99**(10): p. 3838-43.
77. Bartholomew, A., et al., *Mesenchymal stem cells suppress lymphocyte proliferation in vitro and prolong skin graft survival in vivo.* Experimental hematology, 2002. **30**(1): p. 42-48.
78. Krampera, M., et al., *Bone marrow mesenchymal stem cells inhibit the response of naive and memory antigen-specific T cells to their cognate peptide.* Blood, 2003. **101**(9): p. 3722-3729.
79. Nauta, A.J., et al., *Mesenchymal stem cells inhibit generation and function of both CD34+-derived and monocyte-derived dendritic cells.* J Immunol, 2006. **177**(4): p. 2080-7.
80. Sotiropoulou, P.A., et al., *Interactions between human mesenchymal stem cells and natural killer cells.* Stem Cells, 2006. **24**(1): p. 74-85.
81. Le Blanc, K., et al., *Mesenchymal stem cells for treatment of steroid-resistant, severe, acute graft-versus-host disease: a phase II study.* The Lancet, 2008. **371**(9624): p. 1579-1586.
82. Le Blanc, K., et al., *Treatment of severe acute graft-versus-host disease with third party haploidentical mesenchymal stem cells.* The Lancet, 2004. **363**(9419): p. 1439-1441.
83. Bentley, G., et al., *A prospective, randomised comparison of autologous chondrocyte implantation versus mosaicplasty for osteochondral defects in the knee.* Journal of Bone & Joint Surgery, British Volume, 2003. **85**(2): p. 223-230.
84. Steadman, J.R., et al., *Outcomes of microfracture for traumatic chondral defects of the knee: average 11-year follow-up.* Arthroscopy: The Journal of Arthroscopic & Related Surgery, 2003. **19**(5): p. 477-484.
85. Brittberg, M., et al., *Treatment of deep cartilage defects in the knee with autologous chondrocyte transplantation.* N Engl J Med, 1994. **331**(14): p. 889-95.
86. Peterson, L., et al., *Autologous chondrocyte transplantation biomechanics and long-term durability.* The American Journal of Sports Medicine, 2002. **30**(1): p. 2-12.

87. Minas, T., et al., *Increased failure rate of autologous chondrocyte implantation after previous treatment with marrow stimulation techniques.* The American journal of sports medicine, 2009. **37**(5): p. 902-908.
88. Dashtdar, H., et al., *A preliminary study comparing the use of allogenic chondrogenic pre-differentiated and undifferentiated mesenchymal stem cells for the repair of full thickness articular cartilage defects in rabbits.* Journal of Orthopaedic Research, 2011. **29**(9): p. 1336-1342.
89. Qi, Y., et al., *The restoration of full-thickness cartilage defects with mesenchymal stem cells (MSCs) loaded and cross-linked bilayer collagen scaffolds on rabbit model.* Molecular biology reports, 2012. **39**(2): p. 1231-1237.
90. Zscharnack, M., et al., *Repair of chronic osteochondral defects using predifferentiated mesenchymal stem cells in an ovine model.* The American journal of sports medicine, 2010. **38**(9): p. 1857-1869.
91. Haleem, A.M., et al., *The Clinical Use of Human Culture–Expanded Autologous Bone Marrow Mesenchymal Stem Cells Transplanted on Platelet-Rich Fibrin Glue in the Treatment of Articular Cartilage Defects A Pilot Study and Preliminary Results.* Cartilage, 2010. **1**(4): p. 253-261.
92. Choi, K.M., et al., *Effect of ascorbic acid on bone marrow-derived mesenchymal stem cell proliferation and differentiation.* J Biosci Bioeng, 2008. **105**(6): p. 586-94.
93. Chojkier, M., et al., *Stimulation of collagen gene expression by ascorbic acid in cultured human fibroblasts. A role for lipid peroxidation?* Journal of Biological Chemistry, 1989. **264**(28): p. 16957-16962.
94. Hayman, E.G., et al., *Vitronectin—a major cell attachment-promoting protein in fetal bovine serum.* Experimental cell research, 1985. **160**(2): p. 245-258.
95. Lev, R. and S. Spicer, *Specific staining of sulphate groups with alcian blue at low pH.* Journal of Histochemistry & Cytochemistry, 1964. **12**(4): p. 309-309.
96. Green, M.R. and J.V. Pastewka, *Simultaneous differential staining by a cationic carbocyanine dye of nucleic acids, proteins and conjugated proteins II. Carbohydrate and sulfated carbohydrate-containing proteins.* Journal of Histochemistry & Cytochemistry, 1974. **22**(8): p. 774-781.
97. Lecroisey, A. and B. Keil, *Differences in the degradation of native collagen by two microbial collagenases.* Biochem J, 1979. **179**(1): p. 53-8.
98. Seyednejad, H., et al., *Coaxially electrospun scaffolds based on hydroxyl-functionalized poly (ε-caprolactone) and loaded with VEGF for tissue engineering applications.* Biomacromolecules, 2012. **13**(11): p. 3650-3660.
99. Souza, G.R., et al., *Three-dimensional tissue culture based on magnetic cell levitation.* Nat Nanotechnol, 2010. **5**(4): p. 291-6.
100. Kelm, J.M., et al., *Method for generation of homogeneous multicellular tumor spheroids applicable to a wide variety of cell types.* Biotechnology and bioengineering, 2003. **83**(2): p. 173-180.
101. Ivascu, A. and M. Kubbies, *Rapid generation of single-tumor spheroids for high-throughput cell function and toxicity analysis.* Journal of biomolecular screening, 2006. **11**(8): p. 922-932.
102. Kuroda, Y., et al., *Isolation, culture and evaluation of multilineage-differentiating stress-enduring (Muse) cells.* Nature protocols, 2013. **8**(7): p. 1391-1415.
103. Singer, V.L., et al., *Characterization of PicoGreen reagent and development of a fluorescence-based solution assay for double-stranded DNA quantitation.* Analytical biochemistry, 1997. **249**(2): p. 228-238.
104. Sabiston, P., M.E. Adams, and Y.A. Ho, *Automation of 1,9-dimethylmethylene blue dye-binding assay for sulfated glycosaminoglycans with application to cartilage microcultures.* Anal Biochem, 1985. **149**(2): p. 543-8.
105. Vogeser, M. and K. Parhofer, *Liquid chromatography tandem-mass spectrometry (LC-MS/MS)--technique and applications in endocrinology.* Experimental and clinical

endocrinology & diabetes: official journal, German Society of Endocrinology [and] German Diabetes Association, 2007. **115**(9): p. 559-570.
106. Knudson, W., et al., *CD44-anchored hyaluronan-rich pericellular matrices: an ultrastructural and biochemical analysis.* Experimental cell research, 1996. **228**(2): p. 216-228.
107. Almeida, H.V., et al., *Coupling Freshly Isolated CD44+ Infrapatellar Fat Pad-Derived Stromal Cells with a TGF-β3 Eluting Cartilage ECM-Derived Scaffold as a Single-Stage Strategy for Promoting Chondrogenesis.* Advanced healthcare materials, 2015.
108. Baksh, D., R. Yao, and R.S. Tuan, *Comparison of proliferative and multilineage differentiation potential of human mesenchymal stem cells derived from umbilical cord and bone marrow.* Stem cells, 2007. **25**(6): p. 1384-1392.
109. Espagnolle, N., et al., *CD146 expression on mesenchymal stem cells is associated with their vascular smooth muscle commitment.* Journal of cellular and molecular medicine, 2014. **18**(1): p. 104-114.
110. Chen, D., M. Zhao, and G.R. Mundy, *Bone morphogenetic proteins.* Growth factors, 2004. **22**(4): p. 233-241.
111. Gründer, T., et al., *Bone morphogenetic protein (BMP)-2 enhances the expression of type II collagen and aggrecan in chondrocytes embedded in alginate beads.* Osteoarthritis and cartilage, 2004. **12**(7): p. 559-567.
112. Sailor, L.Z., R.M. Hewick, and E.A. Morris, *Recombinant human bone morphogenetic protein-2 maintains the articular chondrocyte phenotype in long-term culture.* Journal of orthopaedic research, 1996. **14**(6): p. 937-945.
113. Steck, E., et al., *Induction of intervertebral disc–like cells from adult mesenchymal stem cells.* Stem Cells, 2005. **23**(3): p. 403-411.
114. Tang, Q.O., et al., *TGF-β3: A potential biological therapy for enhancing chondrogenesis.* 2009.
115. Wrana, J.L., et al., *TGFβ signals through a heteromeric protein kinase receptor complex.* Cell, 1992. **71**(6): p. 1003-1014.
116. Lopez-Casillas, F., J.L. Wrana, and J. Massagué, *Betaglycan presents ligand to the TGFβ signaling receptor.* Cell, 1993. **73**(7): p. 1435-1444.
117. Shen, B., et al., *BMP-2 Enhances TGF-β3–Mediated Chondrogenic Differentiation of Human Bone Marrow Multipotent Mesenchymal Stromal Cells in Alginate Bead Culture.* Tissue Engineering Part A, 2008. **15**(6): p. 1311-1320.
118. Ma, H.L., et al., *Chondrogenesis of human mesenchymal stem cells encapsulated in alginate beads.* Journal of Biomedical Materials Research Part A, 2003. **64**(2): p. 273-281.
119. Lee, S.Y., T. Niikura, and A.H. Reddi, *Superficial zone protein (lubricin) in the different tissue compartments of the knee joint: modulation by transforming growth factor beta 1 and interleukin-1 beta.* Tissue Engineering Part A, 2008. **14**(11): p. 1799-1808.
120. Longobardi, L., et al., *Effect of IGF-I in the chondrogenesis of bone marrow mesenchymal stem cells in the presence or absence of TGF-beta signaling.* J Bone Miner Res, 2006. **21**(4): p. 626-36.
121. Rocha, B., et al., *Secretome analysis of human mesenchymal stem cells undergoing chondrogenic differentiation.* Journal of proteome research, 2014. **13**(2): p. 1045-1054.
122. Chen, X., et al., *Chondrogenic Differentiation Alters the Immunosuppressive Property of Bone Marrow-Derived Mesenchymal Stem Cells, and the Effect Is Partially due to the Upregulated Expression of B7 Molecules.* Stem Cells, 2007. **25**(2): p. 364-370.
123. Ryan, A.E., et al., *Chondrogenic differentiation increases antidonor immune response to allogeneic mesenchymal stem cell transplantation.* Molecular Therapy, 2014. **22**(3): p. 655-667.
124. Technau, A., et al., *Adipose tissue-derived stem cells show both immunogenic and immunosuppressive properties after chondrogenic differentiation.* Cytotherapy, 2011. **13**(3): p. 310-317.

125. Haglund, L., et al., *Proteomic analysis of the LPS-induced stress response in rat chondrocytes reveals induction of innate immune response components in articular cartilage.* Matrix Biology, 2008. **27**(2): p. 107-118.
126. Jakobsen, R.B., et al., *Analysis of the Effects of Five Factors Relevant to In Vitro Chondrogenesis of Human Mesenchymal Stem Cells Using Factorial Design and High Throughput mRNA-Profiling.* PloS one, 2014. **9**(5): p. e96615.
127. Osawa, A., et al., *Activation of genes for growth factor and cytokine pathways late in chondrogenic differentiation of ATDC5 cells.* Genomics, 2006. **88**(1): p. 52-64.